

Analysis of Baffles Design for Limiting Fluid Slosh in Partly Filled Vehicle  
Tanks

Thileepan- Kandasamy

A Thesis

In

The Department

Of

Mechanical and Industrial Engineering

Presented in Partial Fulfillment of the Requirements  
For the Degree of Master of Applied Science (Mechanical Engineering) at  
Concordia University  
Montreal, Quebec, Canada

November 2008

© Thileepan Kandasamy, 2008



Library and Archives  
Canada

Published Heritage  
Branch

395 Wellington Street  
Ottawa ON K1A 0N4  
Canada

Bibliothèque et  
Archives Canada

Direction du  
Patrimoine de l'édition

395, rue Wellington  
Ottawa ON K1A 0N4  
Canada

*Your file* *Votre référence*  
ISBN: 978-0-494-63288-8  
*Our file* *Notre référence*  
ISBN: 978-0-494-63288-8

**NOTICE:**

The author has granted a non-exclusive license allowing Library and Archives Canada to reproduce, publish, archive, preserve, conserve, communicate to the public by telecommunication or on the Internet, loan, distribute and sell theses worldwide, for commercial or non-commercial purposes, in microform, paper, electronic and/or any other formats.

The author retains copyright ownership and moral rights in this thesis. Neither the thesis nor substantial extracts from it may be printed or otherwise reproduced without the author's permission.

**AVIS:**

L'auteur a accordé une licence non exclusive permettant à la Bibliothèque et Archives Canada de reproduire, publier, archiver, sauvegarder, conserver, transmettre au public par télécommunication ou par l'Internet, prêter, distribuer et vendre des thèses partout dans le monde, à des fins commerciales ou autres, sur support microforme, papier, électronique et/ou autres formats.

L'auteur conserve la propriété du droit d'auteur et des droits moraux qui protègent cette thèse. Ni la thèse ni des extraits substantiels de celle-ci ne doivent être imprimés ou autrement reproduits sans son autorisation.

---

In compliance with the Canadian Privacy Act some supporting forms may have been removed from this thesis.

While these forms may be included in the document page count, their removal does not represent any loss of content from the thesis.

Conformément à la loi canadienne sur la protection de la vie privée, quelques formulaires secondaires ont été enlevés de cette thèse.

Bien que ces formulaires aient inclus dans la pagination, il n'y aura aucun contenu manquant.

  
**Canada**

## ABSTRACT

### ANALYSIS OF BAFFLES DESIGN FOR LIMITING FLUID SLOSH IN PARTLY-FILLED VEHICLE TANKS

Thileepan Kandasamy

Concordia University, 2008

The liquid motion within a partly-filled tank has been associated with reduced overturning limits and braking performance of highway tank trucks. The magnitude of maneuver-induced fluid slosh in a partly-filled tank is strongly dependent upon baffles geometry and baffles layout, apart from many other factors. The conventional lateral baffles can effectively suppress longitudinal fluid slosh induced by a braking or acceleration maneuvers, while their effect on lateral slosh in the roll plane is negligible. Both the overturning limits and braking properties of a partly-filled tank truck could be enhanced through alternate baffles geometry and layout. This dissertation research focuses on the analysis of fluid slosh behavior in a partly-filled tank coupled with different designs of anti slosh baffles. A three-dimensional computational fluid dynamics slosh model is developed for the partly-filled cleanbore, and different designs and layouts of baffled tanks on the basis of the Navier-Stokes equations incorporating the VOF technique. The slosh models are formulated to investigate steady-state as well as transient forces and moments imposed on the container under longitudinal, lateral and combined longitudinal and lateral acceleration fields. A quasi-static model of the partly-filled cleanbore tank is also formulated to examine validity of the dynamic fluid slosh model in terms of steady-state responses. The fluid slosh characteristics are analyzed under different fill volumes corresponding to varying cargo load and subjected to external excitations representing steady-turning, straight-line braking and braking-in-turn maneuvers. The fluid slosh analyses are also carried out to

explore the anti-slosh effectiveness of baffles and to evaluate the effects of baffles design factors, such as baffle curvature, orifice size and shape of the orifice.

Alternate design concepts and orientations of baffles are also explored with goals of limiting both the longitudinal and lateral slosh. Concepts in obliquely placed baffle, partial baffles, and partial baffles arranged in an alternating pattern are proposed and analyzed for their effectiveness in limiting the fluid slosh. The results of the study suggest that obliquely placed baffles could help to limit lateral as well as longitudinal fluid slosh under lateral as well as combined lateral and longitudinal acceleration excitations.

## **ACKNOWLEDGEMENTS**

The author is sincerely grateful to his supervisors Dr. Subhash Rakheja and Dr. A. K. Waizuddin Ahmed for their continued intellectual guidance, encouragement and financial support throughout the course of this research. The author is deeply indebted to his parents and his family members for their continued support and understanding. Furthermore, this work is partly supported by the ministere des Transports du Quebec and the Society l'assurance Automobile du Quebec.

## TABLE OF CONTENTS

List of figures

List of tables

Nomenclature

### CHAPTER 1

#### INTRODUCTION AND LITERATURE REVIEW

1.1 General	1
1.2 Review of the relevent literature	3
1.2.1 Analysis of fluid slosh	4
1.2.2 Method of solution	14
1.3 Scope and objectives of the present investigation	18
1.3.1 Objectives	19
1.4 Structure of the thesis	19

### CHAPTER 2

#### MODEL DEVELOPMENT AND METHOD OF ANALYSIS

2.1 Introduction	21
2.2 Three dimensional quasi-static model	22
2.3 Three dimensional dynamic slosh model	25
2.3.1 Method of solution	27

2.3.2 Turbulance effect	27
2.4 Computation of response characteristics	28
2.4.1 Load shift	29
2.4.2 Slosh forces and moments	30
2.5 Geometry discretization and simulations	31
2.6 Summary	34

## CHAPTER 3

### TRANSIENT SLOSH ANALYSIS OF CONVENTIONAL BAFFLED TANK

3.1 Introduction	35
3.2 Design features of the tank and baffles	36
3.3 Simulation matrix	40
3.4 Performance measures	41
3.5 Model validation	42
3.6 Dynamic fluid slosh forces and moments	45
3.6.1 Responses to lateral acceleration	45
3.6.2 Responses to longitudinal acceleration	46
3.6.3 Responses to simultaneous longitudinal and lateral accelerations	47
3.6.4 Effect of baffle opening area	52
3.6.5 Effect of baffle curvature depth	54
3.6.6 Effect of orifice design	56
3.7 Summary	61

## CHAPTER 4

### TRANSIENT FLUID SLOSH ANALYSES OF OBLIQUE AND PARTIAL BAFFLED TANKS

4.1 Introduction	62
4.2 Design concepts in oblique and partial baffles	63
4.3 Dynamic fluid slosh forces and moments	66
4.3.1 Responses of oblique baffled tanks to lateral acceleration	66
4.3.2 Responses of oblique baffled tanks to longitudinal acceleration	67
4.3.3 Responses of oblique baffled tanks to simultaneous longitudinal and lateral accelerations.	68
4.3.4 Responses of a partial baffled tank to lateral acceleration	72
4.3.5 Responses of a partial baffled tank to a longitudinal acceleration	73
4.3.6 Responses of partial baffled tank configurations to simultaneous longitudinal and lateral accelerations	76
4.4 Summary	80

## CHAPTER 5

### CONCLUSIONS AND RECOMMENDATIONS

5.1 Major contributions of the study	81
5.2 Major conclusions	82
5.3 Recommendations for future works	84

REFERENCES	86
------------	----

## LIST OF FIGURES

Figure 1.1	A conventional transverse baffle	12
Figure 2.1	Steady-state free surface of liquid in a partly-filled clean bore tank subject to longitudinal and lateral acceleration	23
Figure 2.2	Computation of moments due to transient slosh forces from the distributed pressure on the wetted boundary	30
Figure 2.3	Schematics of: (a) clean bore; and (b) baffle tanks	31
Figure 3.1	The geometry of the tank equipped with three conventional lateral baffles	37
Figure 3.2	Schematic illustrations of five different configurations of tank and baffles considered	39
Figure 3.3	A perspective of the tank equipped with lateral baffle with equalizer (Tank configuration 'T2')	39
Figure 3.4	Round ramp-step acceleration excitations: (a) lateral acceleration ( $g_y$ ); and (b) longitudinal acceleration ( $g_x$ )	41
Figure 3.5	Comparisons of steady-state lateral and longitudinal force responses due to dynamic fluid slosh in a clean bore tank and quasi-static (QS) model responses under $g_x = 0.3g$ and $g_y = 0.25g$ : (a) lateral force ( $F_y$ ); and (b) longitudinal Force ( $F_x$ )	44
Figure 3.6	Comparisons of steady-state roll and pitch moment responses due to dynamic fluid slosh in a clean bore tank and quasi-static (QS) model responses under $g_x = 0.3g$ and $g_y = 0.25g$ : (a) roll moment ( $M_x$ ); and (b) pitch moment ( $M_y$ )	44
Figure 3.7	Variations in lateral slosh force and roll moment responses of 40 % filled cleanbore (T1) and baffled (T2 and T3) tanks subject to $g_y = 0.25g$ lateral acceleration: (a) lateral force; and (b) roll moment.	46

Figure 3.8	Time-histories of longitudinal slosh force and pitch moment responses of cleanbore and baffled tanks with 40 % fill level, and subject to $g_x = 0.30g$ : (a) longitudinal slosh force; and (b) pitch moment	47
Figure 3.9	Mean lateral and longitudinal force responses of clean-bore (T1) and baffled tanks (T2, T3 and T4) with 40, 60 and 80 % fill level and subject to $g_y = 0.25$ and $g_x = 0.3$ g: (a) Lateral force ( $F_y$ ); and (b) Longitudinal force ( $F_x$ )	49
Figure 3.10	Time-histories of lateral and longitudinal slosh force responses of cleanbore and baffled tanks with 40 % fill level, and subject to $g_y = 0.25g$ and $g_x = 0.30g$ : (a) lateral slosh force; and (b) longitudinal slosh force.	49
Figure 3.11	Amplification factor (M) for lateral and longitudinal force responses of clean-bore (T1) and baffled tanks (T2, T3 and T4) with 40, 60 and 80 % fill level and subject to $g_y = 0.25$ and $g_x = 0.3$ g: (a) Lateral force M ( $MF_y$ ); and (b) Longitudinal force M ( $MF_x$ )	50
Figure 3.12	Time-histories of roll and pitch moment responses of cleanbore and baffled tanks with 40 % fill level, and subject to $g_y = 0.25g$ and $g_x = 0.30g$ : (a) lateral slosh force; and (b) longitudinal slosh force	51
Figure 3.13	Amplification factor (M) for roll moment response of clean-bore (T1) and baffled tanks (T2, T3 and T4) with 40, 60 and 80 % fill level and subject to $g_y = 0.25$ and $g_x = 0.3$ g.	52
Figure 3.14	Amplification factor (M) for lateral and longitudinal force responses of different orifice size baffled tanks (T2a, T2 and T2b) with 40, 60 and 80 % fill level and subject to $g_y = 0.25$ and $g_x = 0.3$ , $g_y = 0.25$ and $g_x = 0.6$ g: (a) Lateral force M ( $MF_y$ ); and (b) Longitudinal force M ( $MF_x$ )	53

Figure 3.15	Time-histories of roll and pitch moment responses of cleanbore and various orifice size baffled tanks with 40 % fill level, and subject to $g_y = 0.25g$ and $g_x = 0.30g$ : (a) roll moment; and (b) pitch moment	54
Figure 3.16	Curvature depths of single orifice full baffles	55
Figure 3.17	Amplification factors in lateral and longitudinal force, and roll moment responses of different curvature depth baffled tanks (T2c and T2) with 40, 60 and 80 % fill level and subject to $g_y = 0.25$ and $g_x = 0.3$ g: (a) Lateral force ( $MF_y$ ); (b) Longitudinal force ( $MF_x$ ); and (c) Roll moment ( $MM_x$ )	55
Figure 3.18	Time-histories of roll and pitch moment responses of different baffle depth tanks with 40 % fill level, and subject to $g_y = 0.25g$ and $g_x = 0.30g$ : (a) roll moment; and (b) pitch moment	56
Figure 3.19	Time-histories of lateral and longitudinal slosh force responses of different orifice shape baffled tanks with 40 % fill level, and subject to $g_y = 0.25g$ and $g_x = 0.30g$ : (a) lateral slosh force; and (b) longitudinal slosh force	57
Figure 3.20	Time-histories of roll moment responses of different orifice shape baffled tanks subject to $g_y = 0.25g$ and $g_x = 0.30g$ : (a) 40 % fill level; (b) 60 % fill level; (c) 80 % fill level	58
Figure 3.21	Time-histories of pitch moment responses of different orifice shape baffled tanks subject to $g_y = 0.25g$ and $g_x = 0.30g$ : (a) 40 % fill level; (b) 60 % fill level; (c) 80 % fill level	59
Figure 3.22	Comparison of free surface position of liquid cargo in tanks with 0.25 g and 0.3g excitation at 20 sec: (a) 60 % fill level for 'T2'; (b) 60 % fill level for 'T5'; (c) 80 % fill level for 'T2'; and (d) 80% fill level for 'T5'.	60
Figure 4.1	Schematics of the proposed baffles and their arrangements in the tank	65
Figure 4.2	Variations in lateral slosh force and roll moment responses of 40 % filled lateral (T2) and oblique baffled (TO1, TO2 and TO3) tanks subject to $g_y = 0.25g$ lateral acceleration: (a) lateral force; and (b) roll moment	67
Figure 4.3	Variations in longitudinal slosh force and pitch moment	68

responses of 40 % filled lateral (T2) and oblique baffled (TO1, TO2 and TO3) tanks subject to  $g_x = 0.60g$  longitudinal acceleration: (a) longitudinal force; and (b) pitch moment.

- Figure 4.4 Amplification factors of lateral ( $MF_y$ ) and longitudinal ( $MF_x$ ) force responses of lateral (T2) and oblique baffled tanks (TO1, TO2 and TO3) with 40, 60 and 80 % fill level and subject to  $g_y = 0.25$  and  $g_x = 0.3$  g: (a) Lateral force ( $MF_y$ ); and (b) Longitudinal force ( $MF_x$ ). 69
- Figure 4.5 Time-histories of lateral and longitudinal slosh force responses of lateral and oblique baffled tanks with 40 % fill level, and subject to  $g_y = 0.25g$  and  $g_x = 0.30g$ : (a) lateral slosh force; and (b) longitudinal slosh force 70
- Figure 4.6 Amplification factors of roll moment ( $MM_x$ ) responses of lateral (T2) and oblique baffled tanks (TO1, TO2 and TO3) with 40, 60 and 80 % fill level and subject to  $g_y = 0.25$  and  $g_x = 0.3$  g 71
- Figure 4.7 Time-histories of roll and pitch moment responses of lateral and oblique baffled tanks with 40 % fill level, and subject to  $g_y = 0.25g$  and  $g_x = 0.30g$ : (a) roll moment; and (b) pitch moment 71
- Figure 4.8 Variations in lateral slosh force and roll moment responses of 40 % filled lateral (T2) and partial baffled (TP1, TP2 and TP3) tanks subject to  $g_y = 0.25g$  lateral acceleration: (a) lateral force; and (b) roll moment. 72
- Figure 4.9 Time-histories of longitudinal force responses of lateral and partial baffled tanks subject to  $g_x = 0.30g$ : (a) 40 % fill level; (b) 60 % fill level; (c) 80 % fill level 74
- Figure 4.10 Time-histories of pitch moment responses of lateral and partial baffled tanks subject to  $g_x = 0.30g$ : (a) 40 % fill level; (b) 60 % fill level; (c) 80 % fill level 75
- Figure 4.11 Time-histories of lateral and longitudinal slosh force responses of lateral and partial baffled tanks with 40 % fill level, and subject to  $g_y = 0.25g$  and  $g_x = 0.30g$ : (a) lateral slosh force; and (b) longitudinal slosh force 76

Figure 4.12 Time-histories of the roll moment responses of lateral and partial baffled tanks subject  $g_y = 0.25g$  and  $g_x = 0.30g$ : (a) 40 % fill level; (b) 60 % fill level; (c) 80 % fill level 78

Figure 4.13 Time-histories of the pitch moment responses of lateral and partial baffled tanks subject  $g_y = 0.25g$  and  $g_x = 0.30g$ : (a) 40 % fill level; (b) 60 % fill level; (c) 80 % fill level 79

## LIST OF TABLES

Table 2.1	Grid sizes considered in the preliminary simulation cases	32
Table 2.2	Magnitude of longitudinal force responses of preliminary simulations involving different time steps and grid sizes	32
Table 2.3	Magnitude of vertical force responses of preliminary simulations involving different time steps and grid sizes	33

## NOMENCLATURE

$a_x, a_y$	Longitudinal (x), lateral (y) accelerations
$A_c$	Cell area in the concerned plane
$A_w$	Wetted area
c	Cell
cg	Centre of gravity
$F_x, F_y, F_z$	Slosh forces along the longitudinal, lateral and vertical axis
$\bar{F}_x, \bar{F}_y, \bar{F}_z$	Steady state forces along the longitudinal, lateral and vertical axis
g	Gravity acceleration
$g_x, g_y, g_z$	Body forces along the x, y and z axes
$\vec{M}$	Moment vector
$M_x, M_y$	Slosh roll, pitch moment
$\bar{M}_x, \bar{M}_y, \bar{M}_z$	Steady state roll, pitch and yaw moments
$MR_p$	Amplification factor
m	Mass
P	Pressure
$P_c$	Pressure on the wall due to cell 'c'
QS	Quasi-static method

R	Tank radius
$R_p$	Selected response variable
$r_c$	Position vector of cell 'c'
s	Seconds
t	Time
T1	Cleanbore tank
T2	Conventional baffle tank
T2a	Small orifice size baffle tank
T2b	Large orifice size baffle tank
T2c	large curvature baffle tank
T3	Conventional baffle tank (reversed curvature)
T4	Flat baffle tank
T5	Half-circle orifice baffle tank
TO1	30 degree oblique baffle tank
TO2	45 degree oblique baffle tank
TO3	60 degree oblique baffle tank
TP1	Bottom partial baffle tank
TP2	Top partial baffle tank
TP3	Alternate partial baffle tank
$u, v, w$	Liquid velocity components along $x, y$ and $z$ directions
$\nu$	Kinematics viscosity
V	Total liquid volume
$\Omega$	Domain of integration.

VOF	Volume of fluid
X,Y,Z	Longitudinal, lateral and vertical axles of Cartesian coordinate system
$X_{cg}, Y_{cg}, Z_{cg}$	Longitudinal, lateral and vertical coordinates of the liquid cargo mass centre
$x_c, y_c, z_c$	Instantaneous position coordinates of a cell 'c' with respect to mid-point of the tank
$\rho$	Fluid density
Max	Peak value
$\tau$	Period of oscillation

## **CHAPTER 1**

### **INTRODUCTION AND LITERATURE REVIEW**

#### **1.1 GENERAL**

In road tankers, the free surface of liquid cargo may experience large excursions for even very small motions of the container. The resulting load shifts in the roll and pitch planes may considerably endanger the stability and maneuvering quality of the vehicle. This problem is common in fuel tanks of automobiles, aircrafts and large ships and tankers. In tank trucks, significant dynamic load transfers in the roll and pitch planes of the container may occur when the container is partly-filled with liquid cargoes. Liquid slosh induced dynamic load transfers in a moving container play a crucial role in the stability of heavy vehicles transporting bulk liquids. The magnitude of slosh and thus the load transfers in a partially filled liquid cargo tank depends on many factors related to vehicle configuration, tank design and maneuvers. Large amplitude sloshing can be induced when a vehicle undergoes braking, turning and lane change maneuvers. A review of heavy vehicle accidents in the U.S.A and Canada revealed that heavy trucks were involved in 28 % of single vehicle accidents as compared with 19 % of the passenger vehicles [3, 53]. Highway accidents involving heavy vehicles may cause significant amount of property damage, human fatalities and environmental damage when flammable or toxic chemical goods are involved. Ranganathan [20] also reported that there are more than 15 000 rollovers of commercial trucks each year in U.S.A and about 62.67 % of these rollovers involved tractor tank semitrailers.

It has been shown that the handling and stability characteristics of tank vehicles depend on many factors, such as tank geometry, variable center of gravity (c.g) location, liquid fill level, maneuver-induced excitation as well as the design of anti slosh devices. Vast majority of the studies have focused on rollover threshold properties of partly-filled tank vehicles [23,24], while only a few have reported load shifts under braking and braking-in-a- turn maneuver [5, 6]. These studies are mostly based upon kineto static solutions of the invicid fluids, which do not characterize the forces and moments caused by the transient fluid slosh. Furthermore, these do not consider the contributions due to anti-slosh devices, such as transverse baffles, which are commonly used in tank trucks.

With the exception of tank trucks employed in general purpose transportation of bulk liquid cargoes, which require cleaning of the tank, the tank trucks in general employ baffles. Baffles in partly-filled tank trucks help to limit the longitudinal load transfer under braking and braking-in-turn maneuvers. The braking performance of such vehicles could thus be greatly enhanced through use of baffles. Only a limited number of studies have attempted to study the effectiveness of anti-slosh devices in limiting the magnitude of slosh forces and moments, and thus the dynamic load transfers. The majority, however, were limited to experiments with laboratory scale tank models [10, 11]. The anti-slosh effectiveness of a baffle would depend upon its design, and layout, number and location in the tank. The influences of such factors on the dynamic slosh forces and moments, however, have not yet been investigated. This is partly attributable to the complexities associated with integration of elaborate computational fluid dynamic (CFD) models of fluid slosh with the nonlinear vehicle model. Alternatively, the effectiveness of

anti-slosh device may be explored through analyses of fluid slosh in a tank alone subject to representative maneuvers-induced excitations. In recent years, CFD codes have been employed to investigate transient fluid slosh within partly-filled tanks [49]. While a number of CFD models of two and three-dimensional slosh have evolved, only two studies have explored the role of baffles [1, 2].

This dissertation research focuses on the analysis of fluid slosh behavior in a partly-filled tank coupled with different designs of anti slosh baffles. A three-dimensional fluid slosh model of a partly-filled tank is formulated to investigate steady-state as well as transient forces and moments imposed on the container under longitudinal and lateral acceleration fields. The slosh models are formulated for different designs and layouts of baffles. The relative anti-slosh properties of the baffles are presented and discussed in terms of peak longitudinal and lateral slosh forces, and roll and pitch moments.

## **1.2 REVIEW OF THE RELEVANT LITERATURE**

The fluid slosh in partly-filled tank trucks has been investigated using kineto-static, and linear and nonlinear liquid slosh models. The directional dynamics of coupled tank-vehicle systems have also been reported on the basis of kineto-static solution of the fluid motion. These reported studies have been reviewed to formulate the motivation and objectives of the dissertation research. The highlights of the relevant studies are briefly discussed in the following subsections

### **1.2.1 Analysis of fluid slosh**

Fluid slosh refers to movement of the free liquid surface within a partly-filled container in the presence of an external disturbance. Depending on the type of external disturbance, fill level and container shape, the free liquid surface can experience different types of motion. In the context of directional dynamics and stability of highway tank trucks, the issue of liquid slosh involves the estimation of hydrodynamic pressure distribution, slosh forces, slosh moments and natural frequencies of the free liquid surface. These properties directly influence the dynamic stability and directional performance of the moving tank trucks [45]. A number of studies have shown that the magnitude of fluid slosh is strongly influenced by the fill level, external excitation and the tank geometry [1, 3]. Furthermore, different anti slosh methods have been described in a few studies [1, 2]. Studies reporting the effects of these factors are discussed below.

#### FILL LEVEL

The liquid fill volume in a tank directly relates to the fluid inertia and the free surface area. The magnitude of fluid slosh forces and moments are thus directly related to the fill volume. Furthermore, the free surface area is also dependent on the tank geometry. The fill volume effects in the reported studies could thus be coupled with the tank cross-section effects. The reported studies have invariably concluded that the fluid fill level in a tank is the main factor, which affects the natural frequencies of slosh, variation in mass center (c.g) coordinates and the dynamic load transfers [1,16]. The liquid motion within a container exhibits infinite number of natural frequencies, but only a few lowest modes are generally excited by the motion of the container. The majority of the studies on natural frequencies of fluid slosh have focused on the fundamental mode alone [16, 45]. These

have shown that large amplitude of slosh occurs when the frequency of external excitation approaches fundamental natural frequency of fluid slosh [45]. The reported studies have considered containers of different geometry, which may not be applicable to tank trucks. Budiansky [14] analyzed the liquid slosh in partially filled circular canals and spherical tanks subjected to lateral acceleration of the container using the hydrodynamic theory. The study reported the natural frequencies of liquid slosh for various fill depths and concluded that first mode frequency and magnitude of force imposed on the container wall increase with increasing fill level. The increase in the slosh forces, however, would be partly attributable to higher inertia due to a higher fill level.

A number of studies have reported the fundamental slosh frequencies and fluid slosh behavior within partially fill containers of different cross sections [15, 16]. Abramson reported that fundamental slosh frequencies in the roll and pitch planes of a cylindrical tank with flat end caps increase with the fill volume. The study reported longitudinal mode frequencies of 0.16, 0.18, 0.21 and 0.26 Hz corresponds to 40, 50, 60 and 80 % fill volume respectively. The corresponds frequencies in the roll plane were 0.56, 0.59, 0.62 and 0.74. It was further shown that the frequencies of slosh in a circular cross-section tank are higher than those in an elliptical tank, which can be attributed to relatively greater width of the elliptical tank.

The fluid slosh in a partly-filled container has also been explored using mechanical equivalent models. Ranganathan [17] employed the pendulum analogy of liquid slosh in a cylindrical tank, originally proposed by Abramson [16], to study the roll

dynamic responses of a tank vehicle under step and sinusoidal lateral excitations. The study concluded that the mean roll dynamic responses of the partially filled tank vehicle are considerably larger than those of an equivalent rigid cargo vehicle. Such findings have also been reported in other studies employing kineto-static fluid slosh [12]. These studies based on kineto-static and mechanical-equivalent fluid slosh models have shown most significant effects of fill volume on the roll dynamic responses, particularly the rollover threshold. On the basis of the quasi static slosh model, it has been reported that the liquid load shift reaches its maximum near the fill level of 70% [1, 12]. This, however, can be considered valid for a particular cross-section tank, and may vary considerably for different tank geometry.

Popov [12] studied the transient slosh response within rectangular and circular cross-section containers, and concluded that the forces and moments due to liquid slosh normalized with respect to the steady state values decrease with increasing fill level. A similar trend was also reported by Modaressi-Tehrani [1] for circular cross-section tank. These studies, however, have reported slosh forces normalized with respect to steady-state magnitudes. The absolute magnitudes of longitudinal and lateral slosh forces, therefore, would increase with the fill volume due to inertia effect. Abramson [16] investigated the fluid slosh within the spacecraft tanks and concluded that the fill level is one of the main factors determining the natural frequency of liquid slosh. It was further reported that the natural frequency of slosh greatly increases for the compartmented tanks, which effectively reduce the characteristic length of the tank. The dynamic fluid slosh and the dynamic behavior of an elastic separating wall in a container were also

investigated in a subsequent study [22], which showed that the natural frequency for rigid wall container is a non linear function of the fill level.

A few studies have also investigated the effect of fill condition on the roll stability limits of the vehicles. Owing to the complexities and high computational demands associated with dynamic fluid slosh analyses; these studies have mostly employed a simplified kineto-static fluid slosh model. Rakheja [23] developed a roll plane model of a circular cross-section tank to study the rollover threshold of a tractor-tank-semi-trailer vehicle when negotiating a steady turn. It was concluded that lower fill levels causes greater lateral load shift leading to proportionally larger overturning moment and thus lower roll stability limit. Further studies following this investigation suggested that some cross-sections are more sensitive to changes in the fill level when rollover is concerned [24].

A few studies have also investigated the effect of fill volume on the transient slosh responses, particularly the lateral and longitudinal forces, and roll moment [1, 12, 25]. Popov [12] investigated two-dimensional slosh in rectangular and cylindrical tanks and reported that fill level not only influences the mean values but also the peak magnitudes of the oscillating forces. The two- and three-dimensional transient fluid slosh analysis of a circular and an optimal cross-section tank, proposed by Kang et al. [28], have also shown significant effect of the fill level on load shifts in the pitch and roll planes of the tank. These studies have shown greater variations in the cargo c.g

coordinates under lower fill volume but larger peak force and moment under higher fill volumes.

### EXTERNAL EXCITATIONS

The maneuver-induced excitations cause fluid slosh and thus the dynamic load transfer in a partly-filled tank truck. The majority of the studies, however, have considered idealized lateral and longitudinal acceleration excitations representing turning and braking, in the form of either step or ramp-step functions. Moreover, the rollover properties of partly-filled vehicles have been greatly emphasized in the reported studies [7, 8, 15, 17]. This may be due to higher frequency of rollover of such vehicles. The rollover property of a vehicle has been mostly defined by its static rollover threshold, defined as the maximum level of lateral acceleration that the vehicle can withstand without overturning under a steady turning maneuver. The magnitudes of the transient fluid slosh and thus the load transfers strongly depend on the severity of the external excitation caused by a braking, turning or braking-in-a-turn maneuver. The dynamic load transfer and variation in the c.g coordinates directly relate to the magnitude of excitation, although the effect is coupled with the tank geometry and the fill volume. The corresponding roll and pitch moments would also increase with input magnitude. Bauer [26] investigated the role of excitation on the magnitude of forces and moment due to hydraulic forces acting on the walls of different tank geometries, and reported that the magnitude of moment is a function of the amplitude of excitation for an upright cylindrical container.

Rakheja et al. [23] analyzed fluid motions inside a partially filled circular tank and reported that lateral forces and roll moment are direct functions of the lateral

excitation imposed on the tank. Subsequently, simplified formulations were proposed to derive the roll moment and rollover threshold of partly-filled vehicles with tank of different cross-sections. Popov [12] further reported that input excitation affects both the peak as well as steady state magnitude of lateral force and turning moment, which were found to be proportional to the magnitude of input excitations. A few studies reporting the slosh responses of baffled and compartmented tanks, also suggest a strong relationship between the overturning moment and the excitation magnitude [1, 11].

Under a longitudinal acceleration excitation, caused by braking, it has been shown that excessive load shift occurs in the pitch plane, which yields greater stopping distances [5]. Kang et al. [25] developed a three dimensional quasi static model of a partly-filled tank coupled with a comprehensive vehicle model to analyze the effects of input excitations on dynamic load transfer. The result suggested that liquid load transfer in the pitch and roll plane increased with input excitations for both circular and optimal tank configurations [3]. When the frequency of the input excitation approaches one of the natural frequencies of the liquid, the large amplitude slosh occurs together with swirling motion of the fluid [1, 27].

### TANK GEOMETRY

The motion of the free surface in a partly-filled tank is greatly influenced by the tank geometry. A number of studies have explored the roll plane motion of the free surface in different cross-section tanks, namely, circular, square, modified oval and elliptic [1,3,8]. It has been shown that for a given fill volume a circular cross-section tank yields relatively higher cg of the cargo compared to the elliptic or modified oval tanks. The

modified oval, elliptic and square cross-section tanks, however, yield large free surface in the roll plane and thus greater load shift and roll moment due to fluid slosh. Kang et al. [28] proposed an alternate optimal cross-section that combines the oval and circular tanks to achieve lower c.g height and lower free surface area under fill volumes exceeding 50 %. It was shown that the optimal cross-section yields higher rollover threshold of the vehicle compared to other cross-section tanks. The reduced free surface in the optimal tank resulted in considerably lower load shift, mass moment of inertia and vehicle roll angle.

The natural frequencies of fluid slosh within a tank also strongly depend on the tank geometry, particularly the cross-section area and the length. Budiansky [14] reported that the natural frequency of free oscillation is influenced by the tank's radius. Bauer [26] also concluded that slosh frequencies and amplitudes of slosh forces and moments are strongly influenced by the geometry of the tank. Apart from the kineto-static solutions, the effect of tank geometry on the transient fluid slosh has been investigated in another study, using a two-dimensional CFD model [29]. The study considered partially filled elliptical tank and proposed optimal aspect ratio of the tank, while the elliptic tanks were found to be less stable compared to rectangular cross section tanks, in the content of a potential vehicle rollover. Ranganathan [20] investigated the roll dynamic performance of partly-filled tank vehicles equipped with four common cross sections: circular, modified oval, modified square and elliptical. The study reported strong influence of tank geometry on the static roll performance of the vehicle and that a modified oval cross section tank yields relatively poor directional performance under partial fill conditions.

## FLUID PROPERTIES

The magnitude of liquid slosh is mostly dependent on the density of fluid and only marginally on the kinematics viscosity of the liquid. The viscosity of commonly transported fluids in general has negligible contribution to the magnitudes of slosh forces and damping [30]. The fundamental slosh frequency and mode shapes are virtually unaffected by liquid viscosity in a range of commonly transported fluids [31, 32]. The fluid density, however, directly affects the fill volume and thus the dynamic load transfers.

## ANTI SLOSH DEVICES

The longitudinal and lateral load transfer caused by fluid slosh in a partly-filled tank can be substantially limited by anti-slosh or slosh damping devices. The tank trucks generally employ transverse baffles, which limit fluid slosh in the longitudinal direction alone. These baffles are designed with a large central orifice and a nearly semi-circular equalizer opening at the bottom, as shown in Figure 1.1. The effects of baffles on the longitudinal and lateral fluid slosh have been investigated in only a few experimental and analytical studies. The studies based on kineto-static solutions of fluid slosh could incorporate only the compartments or separating walls, while the roles of transverse and longitudinal baffles were mostly investigated through laboratory experiments performed on small size scale-model tanks [10, 11]. These have shown that presence of transverse baffles could limit slosh in the longitudinal directions, while the longitudinal baffles limit the lateral load transfers. The longitudinal baffles, however, are not practical due to their excessive weight, which could also interfere with the cleaning tasks.

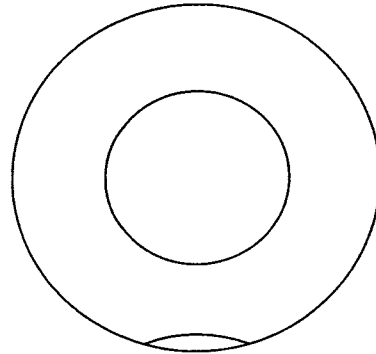


Figure 1.1: A conventional transverse baffle.

A few recent studies have developed two and three-dimension CFD models of partly-filled tanks with baffles to study their anti-slosh effectiveness [1, 2]. These have shown that the fundamental frequency of slosh in the longitudinal mode increases most significantly in the presence of transverse baffles. Sheu and Lee [9] investigated the effect of fill level in the presence of baffles on the slosh behavior in a rectangular oil tanker through formulation of a two dimensional problem and concluded that the baffles geometry in conjunction with the fill level influence the natural frequency of the liquid. It was further demonstrated that the magnitude of wave height under a harmonic excitation resonance frequencies are different for different fill levels. The effectiveness of baffles, however, would depend on their geometry, spacing, and orifice size and location with respect to the free surface. Lloyd et al. [10] experimentally investigated various baffles, including solid dished, oblique, spiral, round, and perforated designs, and concluded that the lightweight perforated baffle could serve as the best anti slosh device.

The effect of size and location of baffle orifice on the slosh has been reported in two studies involving rectangular [11] and oval [2] cross-section tanks. The results

showed comparable magnitudes of slosh forces and moments when orifice opening ranged from 8 to 20 % of the cross-section area. Modaressi-Tehrani [1] reported that lateral baffles have negligible effect on the roll plane load transfer but most significant effect in the pitch plane slosh. Yan [2] investigated the effects of equalizer and alternate baffle designs on the magnitude of transient slosh force and moments, and concluded that the equalizer has negligible effect on liquid slosh, while a multi orifice baffle behaves similar to the conventional single orifice baffles.

Apart from the baffles, closed separating walls have been considered to be most effective in inhibiting the slosh amplitude. Berlamont [4] reported that the optimal compartment length is the half length of the free surface wave. Wang et al. [5] studied the influence of number and size of compartments on the longitudinal load transfer and braking performance of a partly-filled tractor-tank-semitraiter combination, and concluded that equally spaced compartments yield minimum longitudinal load shift under straight-line braking maneuvers, irrespective of the fill level. A few studies have applied the non linear fluid slosh model was applied to determine the liquid dynamic behavior inside a rectangular tank equipped with baffles and compartments [11, 12]. The results attained for long and short containers revealed the existence of a particular fill level for each configuration that would yield considerably lower magnitude of the overturning moment, while the addition of compartment resulted in significantly lower roll moment, especially under higher fill levels. The use of closed separating walls however adds excessive weight and causes difficulties during cleaning and loading or unloading operations.

### 1.2.2 Methods of solution

The fluid slosh within partly-filled tanks has been analyzed using different methods. These include numerical, quasi-static, mechanical analogy and experimental methods. Only a few experimental studies have been reported on fluid slosh within partly-filled moving containers. These studies have contributed greatly to understand of the nature of fluid slosh within fixed contains, while providing essential data for validations of the computational models. Most of these studies, however, have been limited to small scale-tanks and harmonic input excitations. Moreover, the dynamic similarity of the scaled tanks could not be established. The nonlinearity of fluid slosh was experimentally studied by Abramson et al. [13] for vertically placed small scale cylindrical and spherical tanks. The liquid free surface displacements and forces were measured using height transducers and strain sensors, respectively. Fluid slosh in both cylindrical and spherical tanks were investigated for the cleanbore design, and with a vertical splitter plate installed in a direction parallel to the excitation in order to reduce the complex swirl motion in the vicinity of the resonance frequency. The measured data revealed presence of the jump phenomena under excitations near the resonance frequencies, irrespective of the tank geometry. Kobayashi et al. [46] conducted experiments to analyze dynamic liquid slosh responses in horizontal cylindrical tanks, particularly the natural frequency, surface wave height, hydrodynamic pressure and resultant slosh force. The results showed that the maximum slosh forces in the longitudinal and lateral excitation directions occur at 75 and 50 % fill levels, respectively, while the peak magnitudes of longitudinal and lateral forces were reported to be approximately 0.28 and 0.16 times the liquid weight for 80 % fill level, respectively. Furthermore, Pal et al. [47] presented a simple experimental set-up to

measure some of the fundamental sloshing parameters, including slosh frequency, free surface displacement and damping due to slosh within a vertical cylindrical container. The free surface height was detected using 16 position sensors located near the container walls. The measured liquid surface profiles and natural frequencies showed reasonably good agreement with the results obtained from finite element simulations of fluid slosh.

In a recent study, Yan [2] conducted experiment in scale model tank of cross-section, similar to the optimal tank geometry proposed by Kang [3]. The experiments involved analyses of slosh frequencies, and resultant forces and moments due to liquid slosh within the test tank with and without baffles. The experimental results showed that addition of transverse baffles caused a significant increase in longitudinal mode natural frequency, while the lateral mode frequency was not affected. The peak magnitudes of longitudinal slosh force and pitch moment also decreased significantly in the presence of transverse baffles.

The quasi-static (QS) fluid slosh model is a simplified method for predicting the steady-state liquid surface position. In this approach, it is assumed that the fluid is inviscid, while the free surface assumes a straight-line configuration at every instant [1, 3]. This approach neglects contributions due to transient forces and moments that could be large in magnitude. The changes in the coordinates of liquid cargo c.g are computed as a function of the tank geometry, fill level and input excitations, which determines the dynamic load transfers [3]. The quasi-static roll plane models of tank trucks and semitrailers combinations have been developed using the hydrostatic theory to study the

destabilizing effects of shifting cargo on roll stability of the tank vehicles [23, 51]. These models assume negligible contributions due to fluid viscosity and slosh dynamic forces, while fundamental slosh frequency is assumed to be considerably higher than the highest steering frequency. Although the QS models do not predict slosh forces due to free surface oscillations, the computed mean values of the responses revealed reasonably good agreement with the field-measured responses of a scaled tank truck [3].

The liquid slosh within partly-filled containers has been traditionally studied using equivalent mechanical models of the fluid such as an equivalent pendulum model or an equivalent mass–spring model. The forces and moments predicted from the equivalent models could agree reasonably well with the actual hydrodynamic forces and moments when the model parameters are chosen appropriately. Considerable challenges, however, are associated with identifications of parameters of the equivalent mechanical system, which would require comprehensive measurement systems. The methods for calculating model parameters for fluid slosh within rectangular, cylindrical and ellipsoidal tank have been presented by Abramson [13]. Ranganathan et al. [17] used the pendulum theory to model liquid oscillations inside a cylindrical tank. The results showed that the oscillations in roll and lateral acceleration responses of the tank vehicle about the mean values obtained from the quasi-static model, while the magnitudes of oscillations and the transient responses could not be validated.

Numerical methods have been widely used to solve large amplitude fluid slosh within tanks of complex geometry [33, 34]. In these studies, the fluid within the tank is

generally representing by a viscous laminar flow using the incompressible 3-D Navier-Stokes equations, which can be solved through finite difference, finite element method and finite volume methods [40-44]. The approximation of derivatives by finite differences plays a central role in finite difference methods for the numerical solution of differential equations, especially boundary value problems. Finite difference method refers to the discretization of the governing differential equations with the approximation of derivatives using Taylor series expansion. The discretizations are typically based on the structured mesh. It has been suggested that these techniques do not perform well in predicting slosh within a container of complex geometry [39]. The finite element Method is considered to be a good choice for solving partial differential equations over complex domains (such as fluid slosh in tanks, cars and pipelines), particularly when changes in the domain are encountered due to a moving boundary or when the desired precision varies over the entire domain [40]. In the finite volume method, volume integrals in a partial differential equation that contain a divergence term are converted to surface integrals, using the divergence theorem. These terms are then evaluated as fluxes at the surfaces of each finite volume. The finite volume method is advantageous since it is easily formulated to allow for unstructured meshes. The method is used in many computational fluid dynamics packages like FLUENT, including the slosh analyses within tanks of complex geometry.

### **1.3 SCOPE AND OBJECTIVES OF THE PRESENT INVESTIGATION**

From the review of reported studies related to fluid slosh within partly-filled highway tanks, it is apparent that the directional dynamics and stability limits of tank vehicles have been of major concern in view of highway safety. Elaborate analytical models and methods, and experimental setups have been developed for analyses of dynamics of liquid cargo and its interactions with the moving vehicle so as identify directional performance limits of the vehicle. Although the baffles are known to effectively inhibit fluid slosh in the pitch plane, only minimal efforts have been made to study the effects of baffles designs and layouts on the magnitudes of fluid slosh and directional stability of partly filled vehicles. Moreover, the majority of the relevant studies on dynamic fluid slosh have focused on rectangular cross-section tanks. The experimental studies, however, have established considerably knowledge on the role of baffles in partly-filled tanks. Such studies, however, have been based on very small scale laboratory tanks. The contribution due to the boundary effects of small size tanks is not clearly known. Furthermore, the reported experimental and analytical studies on fluid slosh within stationary tanks have considered either transverse or longitudinal baffles with single orifice.

The anti-slosh effectiveness of baffles would depend not only on its geometry but also its location and orientation. Unlike the transverse baffles, an oblique baffle orientation may help limit slosh in both the roll as well as pitch planes. The location of orifice with respect to the free surface would also influence the dynamic load transfers and baffle damping effects, which have not yet been investigated. The scope of the

present dissertation research is thus formulated to investigate anti-slosh effectiveness of alternate baffle designs and layouts. The study aims at analyses of transient fluid forces, moment and magnitudes of load shift as the measures of anti-slosh effect.

### **1.3.1 Objectives**

The primary objective of the dissertation research is to analyses the effect of different baffles designs and layouts on the transient slosh forces and moments caused by fluid slosh in a partly-filled tank. The specific objectives are listed below:

- ❖ Develop a three dimensional CFD fluid slosh model of a clean bore and baffled cylindrical horizontal tank subject to external excitations along the longitudinal and lateral axes.
- ❖ Configure different concepts in anti slosh mechanisms in the pitch and roll planes, such as lateral, partial and oblique baffles.
- ❖ Formulate performance measures that relate to directional performance stability of vehicles, such as forces, moments and load shifts.
- ❖ Investigate anti-slosh effectiveness of different concept and influences of fill levels and magnitude of external excitation.

## **1.4 STRUCTURE OF THE THESIS**

The first chapter presents a brief review of the relevant reported studies. Including the methods of analyses, and main factors affecting the fluid slosh. A detailed CFD model of the partly-filled tank with and without baffles is presented in chapter 2 together with the method of analysis and simulation strategies. Chapter 3 presents the analysis of liquid

slosh inside a partly filled circular cross-section tank with different lateral baffles design parameters, and effects of excitation magnitude and fill level. Chapter 4 presents the simulations results on fluid slosh with different types of baffles, such as transverse, oblique and partial. The influences of main factors such as fill level, magnitude of input excitation and baffle design parameters on the liquid slosh are presented and discussed. The conclusions derived from the study together with major contributions are summarized in chapter 5.

## CHAPTER 2

### MODEL DEVELOPMENT AND METHOD OF ANALYSIS

#### 2.1 INTRODUCTION

Analyses of effect of fluid slosh on the directional dynamic performances of partly-filled highway tank vehicles involve interactions of: (i) liquid cargo with the tank and vehicle structure; (ii) vehicle and the road at the tire-road interfaces; and (iii) driver and the vehicle through execution of steering and braking acceleration maneuvers. Considering the extreme nonlinearities of the vehicle system and the fluid slosh, the analysis of a coupled tank-vehicle system is quite complex and computationally demanding. Such analyses have thus been mostly limited to kineto-static fluid slosh coupled with vehicle models of varying complexities [20, 21]. These models, however, are not applicable for baffled tanks, and neglect contribution due to transient fluid slosh. It has been shown that the forces and moments caused by transient fluid slosh are significantly greater than those predicted by the quasi-static formulations [1, 2].

Thus far, only a few studies have developed analytical models of coupled tank-vehicle system incorporating transient fluid slosh [2, 20, 21]. The interactions between the fluid and the vehicle are incorporated in an iterative manner by interfacing the slosh forces and moments derived from a CFD model of fluid slosh at an instant with the vehicle motion in a successive instant. Furthermore, these studies have incorporated two-dimensional fluid slosh models for tanks without baffles. A three-dimensional fluid slosh

model of a baffled tank was developed and integrated to a pitch-plane vehicle model in recent study [2].

Alternatively, relative anti-slosh effectiveness of different baffles design could be investigated through analysis of a fluid tank model alone. This approach is considered to be computationally efficient compared to the analysis involving the coupled tank vehicle system and would permit analyses of alternative baffle layouts in an effective manner. This chapter presents the formulation of dynamic fluid slosh model of a partly-filled circular cross-section tank with and without baffles to study the effectiveness of baffles. The governing equations together with the boundary conditions representing the liquid motion are described. A kineto-static model is also formulated so as to establish the reference steady-state responses for examining the validity of the dynamic slosh model.

## **2.2 THREE DIMENSIONAL QUASI-STATIC MODEL**

A quasi-static model of a partly-filled tank is initially formulated, as described in [1], to obtain estimates of steady-state slosh forces and moments under lateral and longitudinal acceleration excitations. The resulting slosh forces and moments are subsequently applied to examine validity of the dynamic fluid slosh model in terms of steady-state responses. Considering that the quasi-static models are not applicable for fluid load shift in tanks with baffles, the model is presented for a clean-bore tank alone. The tank vehicles encounter longitudinal as well as lateral forces during steering and braking maneuvers, which cause considerable load shifts in both the roll and pitch planes, when the tank is partly-filled. Assuming quasi static motion of the fluid free surface under application of

longitudinal and lateral accelerations (Figure 2.1), the total pressure differential can be expressed as [3].

$$dP = \frac{\partial P}{\partial x} dx + \frac{\partial P}{\partial y} dy + \frac{\partial P}{\partial z} dz \quad (2.1)$$

where P is fluid pressure.

The force balance on a liquid element in the steady state,

$$g_x = \frac{1}{\rho} \frac{\partial P}{\partial x}, \quad g_y = \frac{1}{\rho} \frac{\partial P}{\partial y}, \quad g_z = -\frac{1}{\rho} \frac{\partial P}{\partial z} \quad (2.2)$$

where  $g_x$ ,  $g_y$  and  $g_z$  are body forces along the x, y and z axes, respectively, and  $\rho$  is fluid density.

The total pressure differential may thus be expressed in the following form,

$$dP = \rho g_x dx + \rho g_y dy + \rho g_z dz \quad (2.3)$$

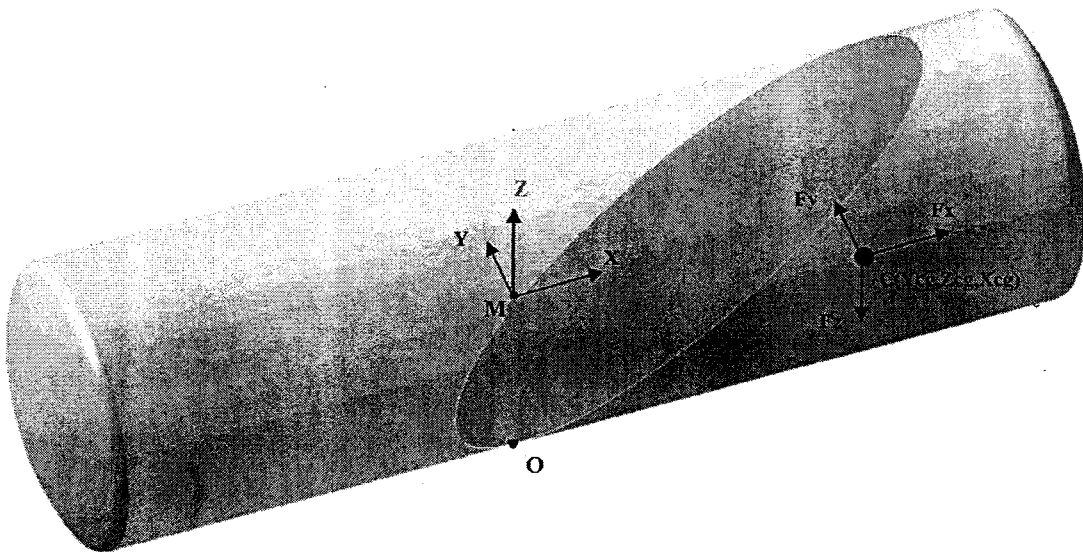


Figure 2.1: Steady-state free surface of liquid in a partly-filled clean bore tank subject to longitudinal and lateral acceleration.

Considering that the pressure at the free surface is uniformly distributed, the three dimensional equation of the free surface at the static condition may be obtained as [1],

$$Y(x,z) = -\frac{g_x}{g_y}x - \frac{g_z}{g_y}z + c_0 \quad (2.4)$$

where  $c_0$  is a constant, which is determined based on the constant fluid volume.

The instantaneous coordinates of the mass center of fluid can be derived from the following volume integrals:

$$X_{cg} = \frac{1}{V} \iiint_V x dv, \quad Y_{cg} = \frac{1}{V} \iiint_V y dv \quad \text{and} \quad Z_{cg} = \frac{1}{V} \iiint_V z dv \quad (2.5)$$

where  $X_{cg}$ ,  $Y_{cg}$  and  $Z_{cg}$  are longitudinal, lateral and vertical coordinates of the liquid cargo mass centre, respectively.  $V$  is total liquid volume and  $v$  defines the domain of integration.

The mass center coordinates directly relate to quasi-static load shift under applications of  $g_x$ ,  $g_y$  and  $g_z$ . The resulting steady state forces can be derived from:

$$\bar{F}_x = mg_x, \quad \bar{F}_y = mg_y, \quad \bar{F}_z = mg_z \quad (2.6)$$

where  $\bar{F}_x$ ,  $\bar{F}_y$  and  $\bar{F}_z$  are steady state forces along the longitudinal, lateral and vertical axis, respectively, and  $m$  is mass of the fluid.

The variations in mass-center coordinates yield considerable roll pitch and yaw moments. Quasi-static roll, pitch and yaw moments about the tank base 'O' (Figure 2.1), can be derived from:

$$\bar{M}_x = Y_{cg} F_z - (Z_{cg} + R) F_y \quad (2.7)$$

$$\bar{M}_y = (Z_{cg} + R) F_x - X_{cg} F_z \quad (2.8)$$

$$\bar{M}_z = X_{cg} F_y - Y_{cg} F_x \quad (2.9)$$

where  $\bar{M}_x$ ,  $\bar{M}_y$  and  $\bar{M}_z$  are steady state roll, pitch and yaw moments, respectively, and  $R$  is the radius of the tank.

### 2.3 THREE DIMENSIONAL DYNAMIC SLOSH MODEL

The motion of an incompressible liquid inside the tank may be represented by the momentum and mass conservation equations. Assuming three-dimensional laminar flow with constant viscosity, the governing equations of fluid flow with respect to an inertial cartesian coordinate system can be expressed as [1]:

$$\frac{\partial u}{\partial t} + u \frac{\partial u}{\partial x} + v \frac{\partial u}{\partial y} + w \frac{\partial u}{\partial z} = -g_x - \frac{1}{\rho} \frac{\partial P}{\partial x} + \nu \left( \frac{\partial^2 u}{\partial x^2} + \frac{\partial^2 u}{\partial y^2} + \frac{\partial^2 u}{\partial z^2} \right) \quad (2.10)$$

$$\frac{\partial v}{\partial t} + u \frac{\partial v}{\partial x} + v \frac{\partial v}{\partial y} + w \frac{\partial v}{\partial z} = -g_y - \frac{1}{\rho} \frac{\partial P}{\partial y} + \nu \left( \frac{\partial^2 v}{\partial x^2} + \frac{\partial^2 v}{\partial y^2} + \frac{\partial^2 v}{\partial z^2} \right) \quad (2.11)$$

$$\frac{\partial w}{\partial t} + u \frac{\partial w}{\partial x} + v \frac{\partial w}{\partial y} + w \frac{\partial w}{\partial z} = -g_z - \frac{1}{\rho} \frac{\partial P}{\partial z} + \nu \left( \frac{\partial^2 w}{\partial x^2} + \frac{\partial^2 w}{\partial y^2} + \frac{\partial^2 w}{\partial z^2} \right) \quad (2.12)$$

and

$$\frac{\partial u}{\partial x} + \frac{\partial v}{\partial y} + \frac{\partial w}{\partial z} = 0 \quad (2.13)$$

Where  $u$ ,  $v$  and  $w$  are the liquid velocity components along  $x$ ,  $y$  and  $z$  directions, respectively,  $P$  is fluid pressure,  $\nu$  is kinematics viscosity of the fluid, and  $g_x$ ,  $g_y$  and  $g_z$  are the unit body forces acting along the  $x$ ,  $y$  and  $z$  directions, respectively. A

homogeneous field of body force has been assumed in the formulations, and momentum and mass conservation equations, which are solved in conjunction with appropriate boundary conditions to compute the velocity components and pressure distribution in the flow domain as a function of time and space. It would be reasonable to assume that the tank is bounded by a rigid wall, which yields that the velocity component normal to the wall is zero at the boundary, implying no-slip boundary condition, such that:

$$\frac{\partial U_T}{\partial n} = 0 \quad (2.14)$$

where  $U_T$  the total velocity of the liquid and  $n$  is the normal directional vector to the boundary.

The deformation of the free surface at each instant of time could be derived assuming irrotational flow with no horizontal displacement of particles at the free surface, which leads to a kinematics restriction in the following form [48]:

$$v = \left( \frac{\partial}{\partial t} + u \frac{\partial}{\partial x} \right) \eta \quad ; \text{ at the free surface} \quad (2.15)$$

where  $\eta$  is the displacement of free surface from its mean position.

The above equation exhibits limitations in analyses, when a folded free surface occurs. The concept of tracking the volume of liquid instead of free surface has thus been widely used. The methodology known as VOF (Volume of Fluid) permits the analysis of deformation of free surface flow through numerical solution techniques [50]. The VOF model is a surface-tracking technique applied to a fixed mesh. It is designed for two or more immiscible fluids where position of the interface between the fluids is of interest. In the VOF model, a single set of momentum equations is shared by the fluids, and the

volume fraction of each of the fluids in each computational cell is tracked throughout the domain.

### **2.3.1 METHOD OF SOLUTION**

The equations of three dimensional fluid flows, satisfying the boundary conditions are solved using the FLUENT software [49]. The VOF method, available within the FLUENT environment, is applied to solve for transient flows involving free surface separation and air within the non filled cross section of the tank. The momentum and mass conservation equations are discretized using finite volume technique considering each cell as a control volume. For transient simulations the governing equations must be discretized in both space and time. The spatial discretization for the time dependent equations is identical to the steady state case. Temporal discretizations involve the integration over a time step. The FLUENT software applies implicit method to solve unsteady free surface flow. The pressure corrector PISO algorithm is selected for solving for transient pressure and velocity responses. The tracking of volume of fluid (VOF) method has been applied to locate the interface between the two fluid phases: liquid and air [51].

### **2.3.2 TURBULANCE EFFECT**

A number of reported studies have considered laminar flow models in solutions of the Navier–Stokes equations, which provided reasonably good correlations with the experimental data [9]. Popov [29] developed a mathematical model of liquid slosh inside a partly-filled circular tank subject to a lateral acceleration field, based on the laminar flow assumption. The laminar flow model was solved for velocity and pressure responses

under a wide range of Reynold's numbers, which corresponded to turbulent flows. The study also performed a series of experiments on a scale model tank of rectangular cross-section and the data were used to identify model coefficients and examine the model validity. The transient solutions compared reasonably well with the experiment data, suggesting validity of the laminar flow assumption for such analyses. Another reported study has suggested that a laminar flow model is adequate for analyses of fluid slosh in baffled and clean bore tanks [9]. This may be due to large inertia forces with respect to the viscous force. The magnitude of viscous forces exerted on the tank wall has been reported to be negligible even for a fluid with a high-dynamic viscosity ( $\mu = 0.98 \text{ kg/ms}$ ) [1]. Furthermore, Bauer [26] showed that only a small portion of the liquid bulk inside the container is involved in the acceleration-induced oscillatory motion. The laminar flow assumption would thus be valid in the formulation of the slosh inside a moving tank.

## **2.4 COMPUTATION OF RESPONSE CHARACTERISTICS**

The distribution of transient fluid pressure acting on the tank wall may provide significant insight into a number of characteristic features related fluid-tank interaction such as stress imposed on the container, peak slosh forces and peak over turning moments. Many studies have been reported that the effect of distributed pressure on the tank structure could be investigated in terms of equivalent forces and moments exerted on the walls [8, 12, 23]. It has been further shown that magnitudes of these forces and moments associated with relative movement of the liquid cargo are considerably larger than those of an equivalent rigid cargo. The reported studies on roll dynamic behavior of partly-filled tank vehicles have invariably concluded that the load shift, often expressed

in terms of deviations in the coordinates of the mass centre directly affects the magnitude of the overturning moment. The motion of the free surface of fluid is thus considered as the most significant factor affecting the vehicle roll stability.

The effect of motion of free surface would be far more significant, when transient response characteristics due to liquid slosh and slosh frequencies are considered. The distributed pressure responses are thus analyzed to derive the instantaneous slosh forces, moments and coordinates of the mass center. The user defined functions (UDF) are subsequently developed to evaluate responses in terms of forces, moments and cg coordinates.

#### 2.4.1 LOAD SHIFT

The dynamic load shift due to sloshing cargo is generally expressed by variations in the instantaneous cg coordinates from the static cg coordinates. The instantaneous coordinates of center of gravity of the liquid (cg) can be obtained from the volume integrals over the liquid phase of the domain. Alternatively, for the discrete mesh, the coordinates are evaluated from:

$$X_{cg} = \frac{\sum_c^{liquid} x_c A_c}{\sum_c^{liquid} A_c} ; \quad Z_{cg} = \frac{\sum_c^{liquid} z_c A_c}{\sum_c^{liquid} A_c} \quad \text{and} \quad Y_{cg} = \frac{\sum_c^{liquid} y_c A_c}{\sum_c^{liquid} A_c} \quad (2.16)$$

Where  $x_c$ ,  $y_c$  and  $z_c$  are instantaneous position coordinates of a cell 'c' with respect to mid-point of the tank, 'M', as shown in Figure 2.1, and the 'liquid' defines the domain of integration.  $A_c$  is the cell area in the concerned plane.

## 2.4.2 SLOSH FORCES AND MOMENTS

The resultant forces acting on the container structure are computed from the distributed pressure acting on the wall. The integration over the wetted area of the wall cells yields:

$$F_x = \sum_c^{A_w} P_c A_c.i \quad ; \quad F_y = \sum_c^{A_w} P_c A_c.j \quad \text{and} \quad F_z = \sum_c^{A_w} P_c A_c.k \quad (2.17)$$

where  $F_x$ ,  $F_y$  and  $F_z$  are the resultant forces acting on the tank wall,  $P_c$  is the pressure on the wall due to cell 'c' and  $A_c$ ,  $A_w$  defines the cell and wetted area respectively.

The pitch, roll and yaw moments due to liquid slosh are computed about the tank base 'O', as shown in Figure 2.1. The moments are computed from the distributed pressure or force acting on the wetted structure boundary and position vector of the individual cells, as shown in the roll plane in Figure 2.2, such that:

$$\vec{M} = \sum (\vec{P}_c A_c) \cdot \vec{r}_c \quad (2.18)$$

Where  $\vec{M}$  is moment vector and  $r_c$  is position vector of cell 'c' with respect to the tank base 'O'.

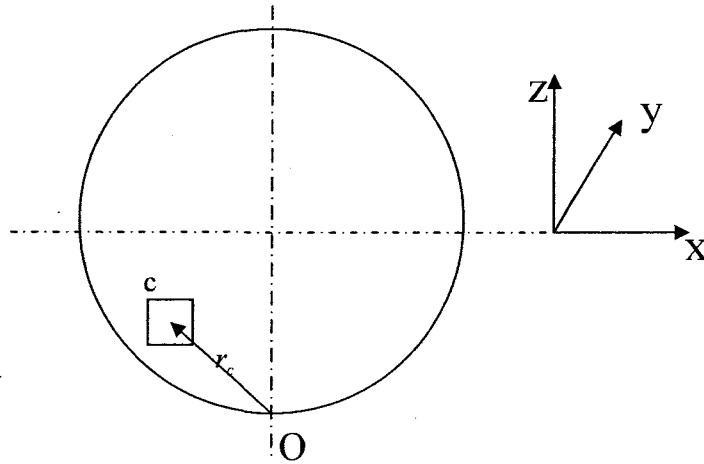


Figure 2.2: Computation of moments due to transient slosh forces from the distributed pressure on the wetted boundary.

## 2.5 GEOMETRY DISCRETIZATION AND SIMULATIONS

Figure 2.3 illustrates the schematics of the cleanbore and baffled tanks, considered for the analyses. Both the tanks comprise curved end caps. The curved baffles are also employed in the baffled tank model. The unstructured meshing scheme was applied using GAMBIT to discretize the fluid domain in the tank. Considering the sensitivity of convergence to the mesh size, three different grid sizes were considered to investigate the effect of the mesh size on the accuracy of the response. These are referred to as 'Grid 1', 'Grid 2' and 'Grid 3'.

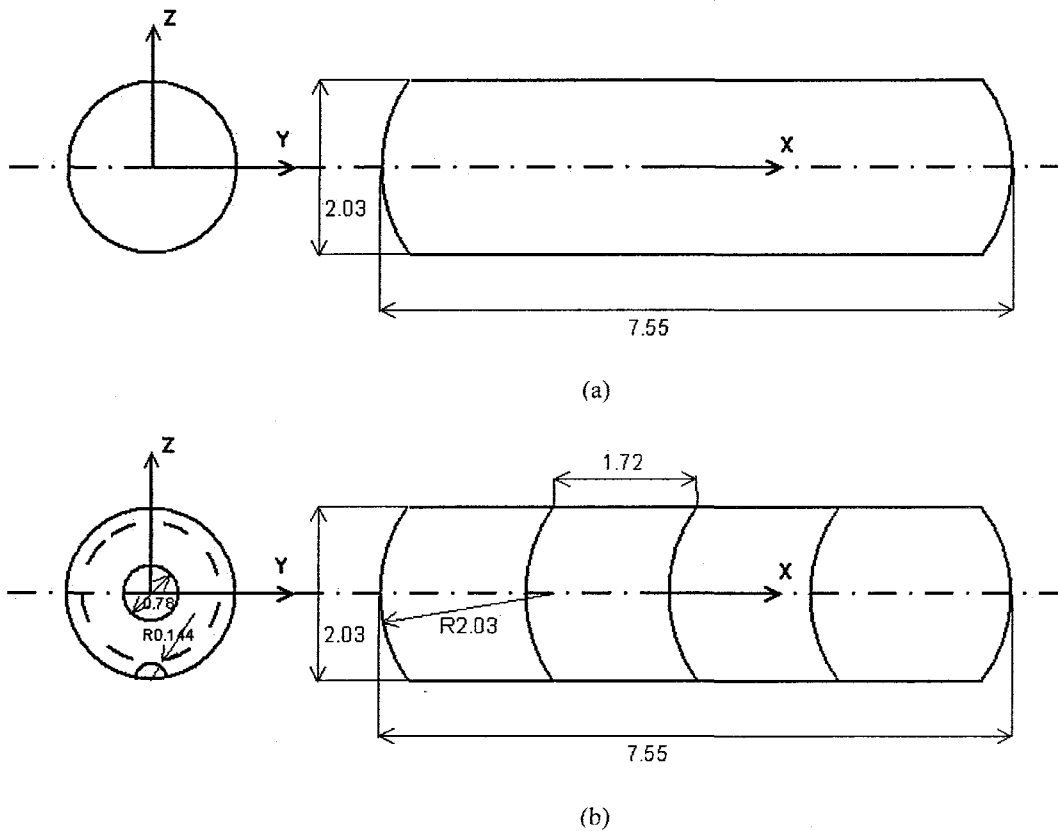


Figure 2.3: Schematics of: (a) clean bore; and (b) baffled tanks

Table 2.1: Grid sizes considered in the preliminary simulation cases

Grid	Number of Cells	Number of faces	Number of nodes
Grid 1	41580	170305	58032
Grid 2	58580	178395	62426
Grid 3	245504	747072	256266

Table 2.1 summarizes the number of cells considered for the three preliminary simulation cases together with the corresponding number of nodes. The ‘Grid 1’ is a coarse mesh of 41,580 cells in the 7.55 m long cleanbore tank, while ‘Grid 3’ is a finer mesh of 245,504 cells. The relative accuracy of convergence of the three mesh sizes were evaluated in terms of steady-state vertical and longitudinal force responses. The analyses were performed for the 50% filled tank subject to 0.4 g constant longitudinal acceleration. The analyses were also performed using four different integration step sizes (0.0001, 0.001, 0.01 and 0.025) to study the effect of the step size on the solutions. Tables 2.2 and 2.3 present the transient longitudinal ( $F_x$ ) and vertical ( $F_z$ ) force responses corresponding to the three grid sizes and four integration step sizes at  $t=2s$ .

Table 2.2: Magnitude of longitudinal force responses of preliminary simulations involving different time steps and grid sizes.

Grid \ Time step (s)	Longitudinal Force at $t=2s$ (N)			
	0.0001	0.001	0.01	0.025
Grid 1	41 716.86	41 642.17	41 413.39	41 490.89
Grid 2	41 516.25	41 418.12	41 040.02	41 140.29
Grid 3	41 624.46	41 524.77	41 241.94	41 296.85

Table 2.3: Magnitude of vertical force responses of preliminary simulations involving different time steps and grid sizes.

Grid \ Time step (s)	Vertical Force at t=2s (N)			
	0.0001	0.001	0.01	0.025
Grid 1	79 173.80	79 242.33	80 721.06	81 464.70
Grid 2	79 743.45	80 019.46	81 231.57	81 873.23
Grid 3	79 524.30	79 892.32	81 206.74	82 012.53

The results suggest slight variations in the transient response with varying grid sizes. The deviations in the responses are also coupled with the time step. The smallest time step (0.0001s) yields least deviations in responses attained with three grid sizes. The considered grid variations, however, yield relative deviations in  $F_x$  and  $F_z$  in the order of 1 % or less. Considering that the computational time is nearly proportional to the mesh size, Grid ‘2’ is considered to yield adequate compromise in accuracy and simulation efficiency. The larger time step (0.025s) was also chosen for further simulations to enhance to computational efficiency.

The 3-D mesh of two-phase fluid domain is imported into the FLUENT software and the segregated method of solution is applied to solve for linearized discrete equations, assuming laminar flow with two phases and primitive variables, namely pressure at the center of each cell and velocity components at the cell faces. First-order upwind and the body-force-weighted schemes are applied for the momentum and pressure correction equations, and spatial components of the governing equations are discretized using a fixed time step and the first-order time advancing scheme. The FLUENT environment also employs PISO algorithm for pressure–velocity coupling [50].

The convergence criteria based on the residual values of 0.0001 was selected in the simulation, while the input excitations were prescribed through user defined functions.

## **2.6 SUMMARY**

A three-dimensional quasi-static liquid slosh model is formulated to determine the steady-state slosh forces and c.g coordinates, which would serve as the reference values of verifying the dynamic fluid slosh model. This model, however, is not applicable for analysis of fluid slosh in baffled tanks. A three-dimensional fluid slosh model is developed in the FLUENT software to study the transient variations in slosh forces and moments, and c.g coordinates for the baffled as well as cleanbore tanks. Preliminary simulations are performed to select appropriate grid size and time step to achieve efficient simulations. The selected grid size and time step are applied to study transient fluid slosh under different excitations in the subsequent chapters.

## CHAPTER 3

### TRANSIENT SLOSH ANALYSIS OF CONVENTIONAL BAFFLED TANK

#### 3.1 INTRODUCTION

The directional dynamic analysis of a partly-filled highway tank vehicle necessitates integration of nonlinear vehicle model with a dynamic fluid slosh model of the partly-filled tank. The coupled vehicle-tank modeling task thus poses considerable challenges and computational demands. Such analyses have been attempted in only few studies [20, 21], which consider two-dimensional fluid slosh in the tank without baffles. The baffles are known to significantly influence the slosh forces and moments, it has experimentally shown that presence of baffles causes three-dimensional fluid slosh even under pure lateral or longitudinal acceleration excitations [10]. The effectiveness of a baffle may depend on its orientation inside the tank, geometry, and number of location. The anti-slosh effectiveness of baffles can be conveniently evaluated through dynamic fluid slosh analyses of the partly-filled tanks alone subject to representative vehicle or structure excitations. Three-dimensional fluid slosh in a partly-filled baffled tank alone has been reported in two recent studies [1, 2], which considered transverse conventional baffles. The effect of design factors such as baffle curvature, orifice size, and location of orifice on the magnitude of transient slosh forces and moments has been investigated in a single study [1] employing the optimal tank cross-section proposed by Kang [3].

In this chapter, the three-dimensional computational fluid dynamic (CFD) model of a full scale circular cross-section tank without and with different types of lateral baffles is formulated and analyzed using the method described in chapter 2. The dynamic

fluid slosh within the tank is solved using the VOF method in FLUENT software under lateral, longitudinal and simultaneous lateral and longitudinal excitations. The simulation results are discussed in view of influences of different design parameters, such as baffle curvature, orifice size, shape of the orifice, location of the orifice, magnitude of excitation and fill level on the resulting slosh forces and moments. The dynamic response characteristics are evaluated in terms of instantaneous load shift and slosh forces and moments in the three-dimensional space. Correlations between the steady-state simulation results and those derived from quasi-static solutions are also discussed.

### **3.2 DESIGN FEATURES OF THE TANK AND BAFFLES**

A 7.55 m long circular cross-section tank of 1.015m radius and 25.525  $m^3$  volume is considered for the analyses. The full load capacity of the tank is approximately 22 000 kg assuming a full load of gasoline ( $\rho = 850kg/m^3, \nu = 0.0687kg/ms$ ). The geometry is considered adequate for a three or four-axle straight tank in accordance with the current weights and dimensional regulations (CFR code 148.346-2, which addresses the institution of ASME section 8 Dev. 1 UG32). The origin of the coordinate system used is located at the geometric centre of the tank. The moments due to fluid slosh, however, calculated with respect to the projection of the geometric centre at the bottom of the tank, point 'O', as shown in Figure 3.1, using the distributed pressure responses as described in Eq. (2.18). The geometry of the baffles bulkheads is chosen in accordance with CFR codes and ASME guidelines. Three nearly equally-spaced baffles are considered, and each baffle is provided with an equalizer at the bottom with total area being 1 % of the tank cross section area, as shown in Figure 3.1.

The CFD models are formulated for five different tank and baffle configurations. These include: (i) a cleanbore un baffled tank, referred to as tank 'T1' and shown in Figure 3.2(a); (ii) tank with three conventional baffles with spherical curvature opposite to the flow direction under a braking input as shown in Figure 3.2(b), referred to as tank 'T2'; (iii) same as tank T2 but baffle curvature in the flow direction, as shown in Figure 3.2(c) and referred to as tank 'T3'; (iv) a tank with flat lateral baffles, as shown in Figure 3.2(d) and referred to as tank 'T4'; and (v) the tank equipped with half-circle orifice baffles; as shown in Figure 3.2(e), referred to as tank 'T5'. The configurations 'T2' to 'T4' employ baffles with a large central orifice within opening area of 12% of the total tank cross-section area. The configuration 'T5' employs baffles with semi-circular orifice of identical opening area. The curvature of baffles employed in tanks 'T2', 'T3' and 'T5' is identical to that of the tank heads. The longitudinal spacing between the baffles is in the order of 1.72 m, which is less than the maximum baffle spacing specified in the above CFR code. The depth of curvature of the heads and baffles in configurations 'T2' and 'T3' is 0.35 m. Figure 3.3 illustrate a perspective of the tank with conventional lateral baffles (configuration 'T2') with equalizer.

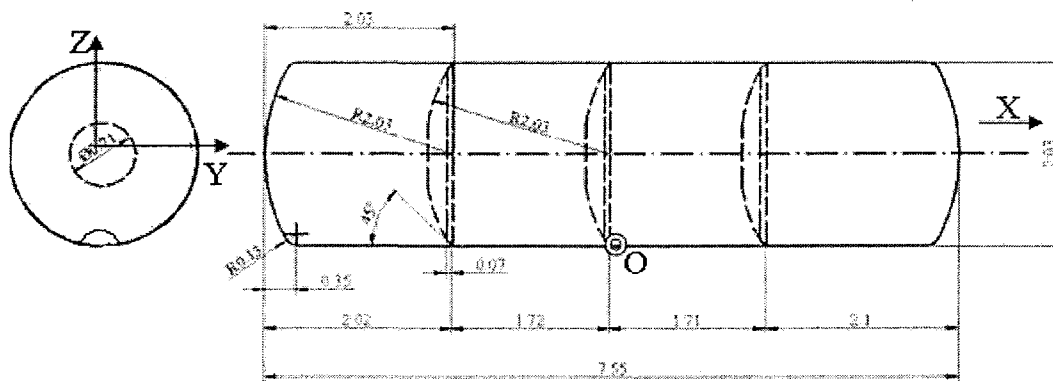
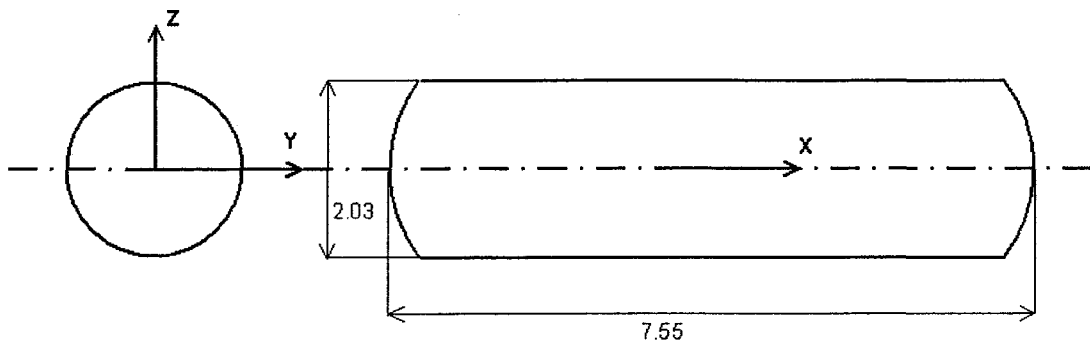
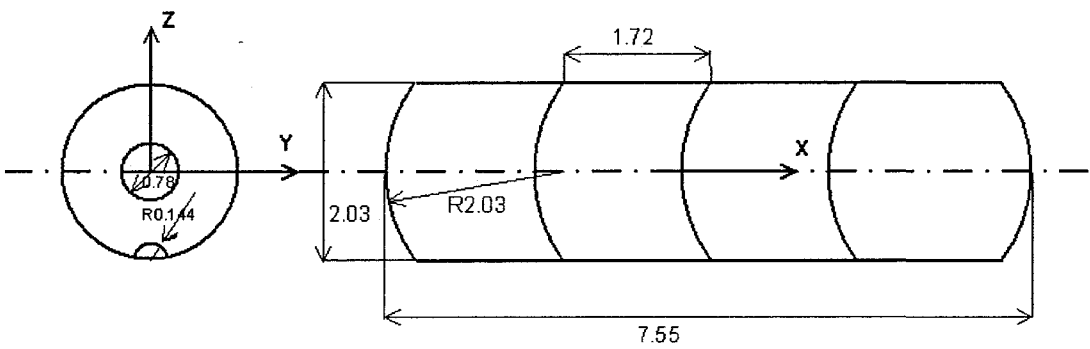


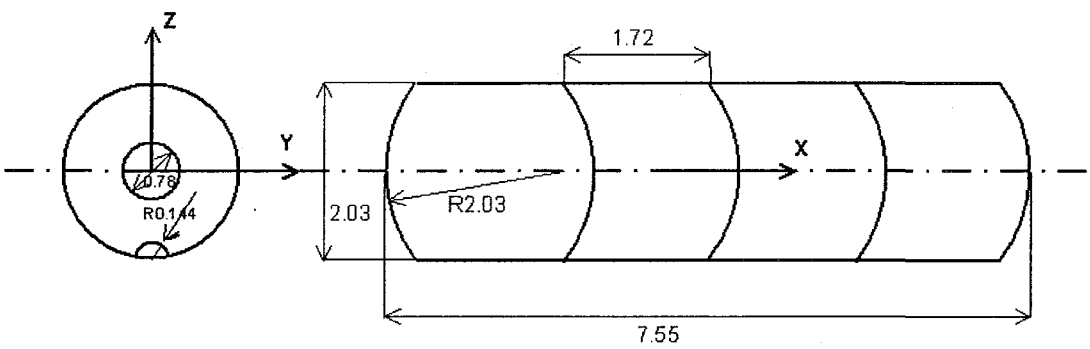
Figure 3.1: The geometry of the tank equipped with three conventional lateral baffles



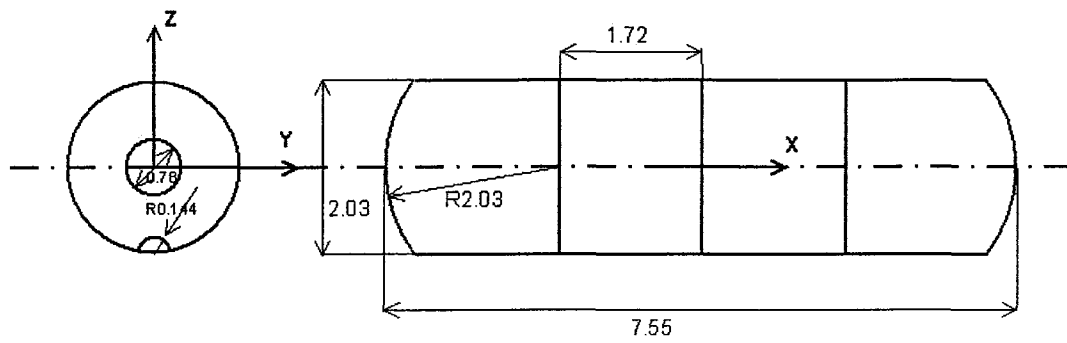
(a) Cleanbore tank 'T1'



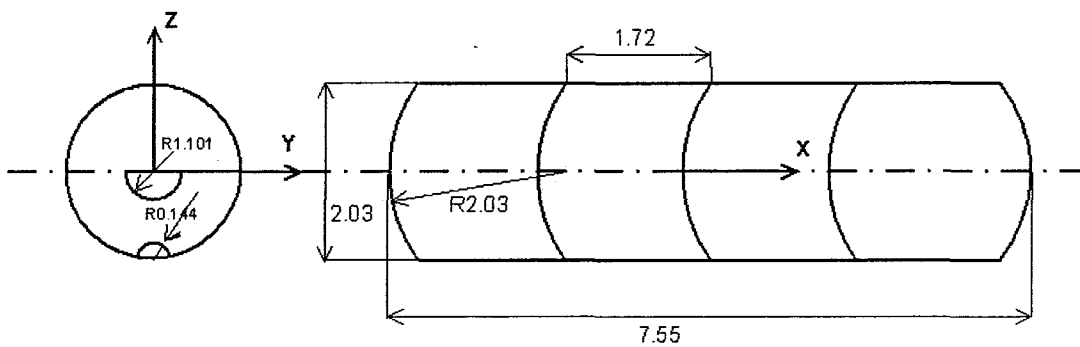
(b) Conventional baffle tank 'T2'



(c) Conventional baffle tank 'T3'



(d) Flat baffle tank 'T4'



(e) Half-circle orifice baffle tank 'T5'

Figure 3.2: Schematic illustrations of five different configurations of tank and baffles considered.

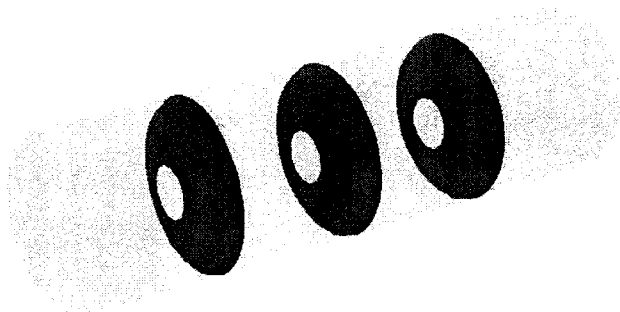


Figure 3.3: A perspective of the tank equipped with lateral baffle with equalizer (Tank configuration 'T2').

### 3.3 SIMULATION MATRIX

The simulations are performed to investigate the effect of different baffle configurations (Figure 3.2), fill volume, and magnitude and direction of acceleration excitations. The highway tanks may transport a wide range of liquid products of varying mass density, which could lead to partial fill conditions. Moreover, vehicles employed in local deliveries of fuel oils may also carry partial loads. An analysis of dynamic fluid slosh within the tanks with different fill levels is thus essential to explore the effectiveness of baffles. In this present study, three different fill levels of fuel ( $\rho = 850 \text{ kg/m}^3, \nu = 0.0687 \text{ kg/ms}$ ) are considered. These include a low (40%), intermediate (60%) and high (80%) fill levels. The fill percentage level is defined as the ratio of the fill height from the bottom of the tank to the tank diameter. The three fill levels correspond to fluid volumes of 10.21, 15.315 and  $20.42 \text{ m}^3$ , respectively, and cargo loads of 8678.5, 13 017.75 and 17 357 kg.

The simulations were performed under three different excitations: a constant lateral acceleration representing steady-turn maneuvers; a constant longitudinal acceleration representing straight line braking; and simultaneous lateral and longitudinal acceleration representing a braking-in-a-turn maneuver. Rounded ramp-step variations in acceleration excitations are considered, as shown in Figure 3.4, in order to minimize the transient flow oscillation caused in the vicinity of the discontinuity [1]. Different magnitudes of lateral and longitudinal acceleration excitations are also considered to study the role of maneuvers on the fluid slosh in cleanbore and baffled tanks. For this purpose, lateral acceleration ( $g_y = 0.25g$ ), and two different magnitude of longitudinal

acceleration ( $g_x=0.3g$  and  $0.6g$ ) are selected. The simulations under combined lateral and longitudinal acceleration involved:  $g_x = 0.3g$  and  $g_y = 0.25g$ ; and  $g_x = 0.6g$  and  $g_y = 0.25g$ .

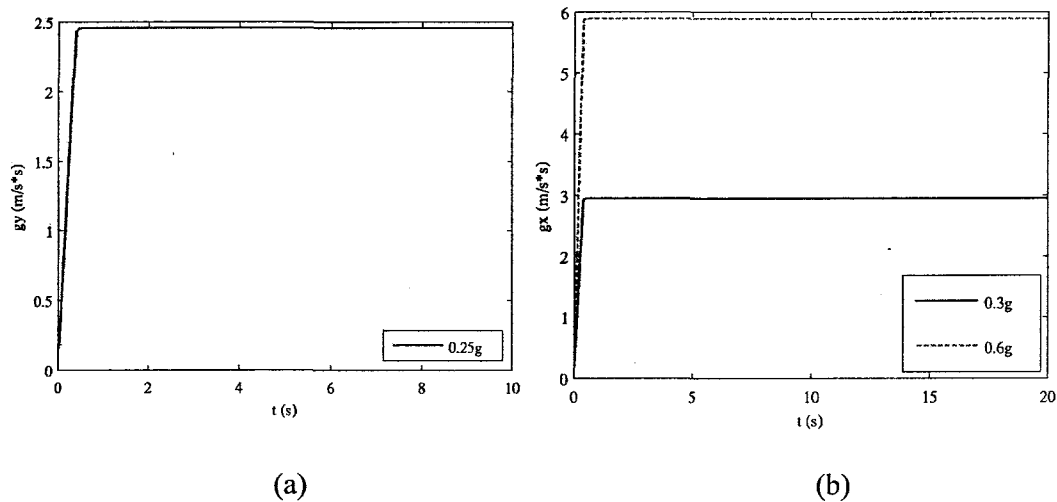


Figure 3.4: Round ramp-step acceleration excitations: (a) lateral acceleration ( $g_y$ ); and (b) longitudinal acceleration ( $g_x$ )

### 3.4 PERFORMANCE MEASURES

The directional dynamic performance of a partly filled tank truck is directly influenced by the forces and moments induced by the sloshing cargo apart from those induced by tire-road interactions. The relative performance potentials of different baffle and tank configurations are thus evaluated in terms of longitudinal and lateral forces, and pitch and roll moments imposed by the sloshing liquid. The steady-state as well as transient responses of different configurations are evaluated to assess performance in terms of steady-state and peak forces and moments. The deviations in the dynamic response values from the corresponding steady-state solutions are quantified in the form of

amplification factors, defined as the ratio of the peak value of the dynamic response quantity to the corresponding mean response, such that [1]:

$$MR_p = \frac{Max(R_p)}{\bar{R}_p} \quad (3.1)$$

Where  $R_p$  is the selected response variable and Max refers to its peak value, and  $\bar{R}_p$  is the mean value.  $MR_p$  is the amplification factor, which defines the peak amplification of the response variable in the transient state with respect to the steady solution, and thus characterizes the transient nature of the oscillatory slosh forces and moments. The mean response quantity is chosen as the normalizing factor, which is known to be close to the steady-state solutions [1, 2]. The mean value  $\bar{R}_p$  is obtained by evaluating the time integral of the response  $R_p$  over duration  $(t_2 - t_1)$ .

$$\bar{R}_p = \frac{1}{t_2 - t_1} \int_{t_1}^{t_2} R_p(t) dt \quad ; \quad \text{for} \quad t_2 - t_1 \gg n\tau \quad (3.2)$$

where  $t_1$  and  $t_2$  define the integration period, which comprises  $n$  ( $>1$ ) cycles of oscillations, and  $\tau$  is the period of oscillation. For the simulation time of 20 s considered in this study, the integration periods varied from 12 to 18 s.

### 3.5 MODEL VALIDATION

The analysis of the transient dynamic model was performed using the selected mesh size and step size as described in chapter 2, for each tank configuration. The steady-state slosh

force and moment responses are compared to those derived from quasi-static formulation presented in section 2.2 in order to examine the model validity. Since the quasi-static formulations are valid only for cleanbore tanks, the comparisons are limited only to tank 'T1'. The three-dimensional quasi-static and dynamic slosh models of the fluid within a partly-filled cleanbore tank are initially solved under constant magnitudes of simultaneous longitudinal ( $g_x = 0.3$ ) and lateral ( $g_y = 0.25$ ) acceleration excitations for three fill conditions (40, 60 and 80%). The simulations were performed over an extended period of 20 s so as to achieve steady-state values, which were found to be identical to the mean values.

Figure 3.5 illustrates comparisons of the steady-state longitudinal ( $F_x$ ) and lateral ( $F_y$ ) slosh force responses under selected maneuvers with those derived from the quasi-static (QS) analysis. Figure 3.6 illustrates comparisons of resulting roll and pitch moments under simultaneous  $g_x = 0.3g$  and  $g_y = 0.25g$ . The comparisons suggest reasonably good agreements between the steady-state or mean dynamic and the quasi-static responses for all the fill levels considered. Some deviations between the two, however, are also observed, particularly, under intermediate and higher fill levels. The steady-state responses tend to be slightly higher than the corresponding QS responses. The peak deviation was found to be below 4 %. This deviation is attributed to the slightly different fluid volume and fluid mass estimated from the mesh in the fluent model. A higher fill volume yields higher steady-state and QS forces due to higher inertia. Modaressi-Tehrani [1] and Yan [2] also reported that steady-state responses differ slightly from the corresponding quasi-static responses by approximately 5 %.

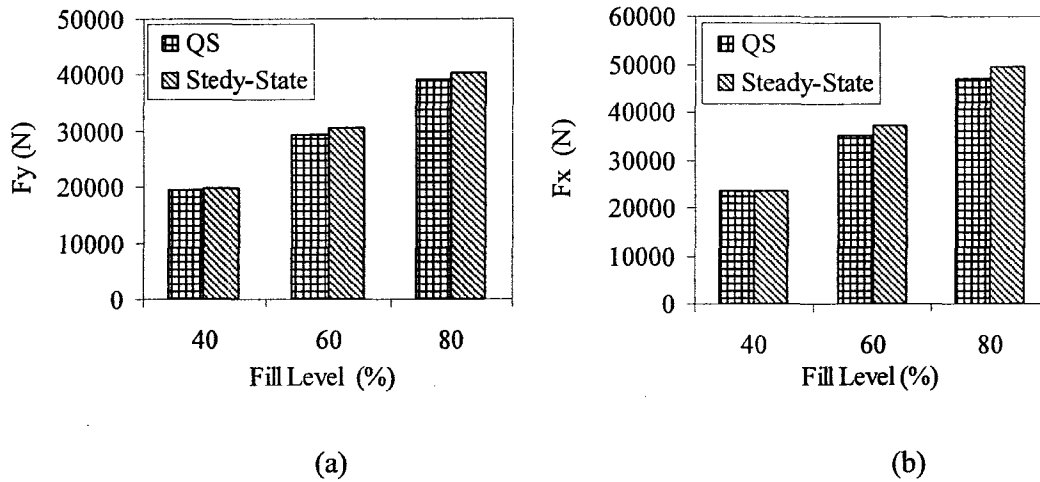


Figure 3.5: Comparisons of steady-state lateral and longitudinal force responses due to dynamic fluid slosh in a clean bore tank and quasi-static (QS) model responses under  $g_x = 0.3g$  and  $g_y = 0.25g$ : (a) lateral force ( $F_y$ ); and (b) longitudinal Force ( $F_x$ ).

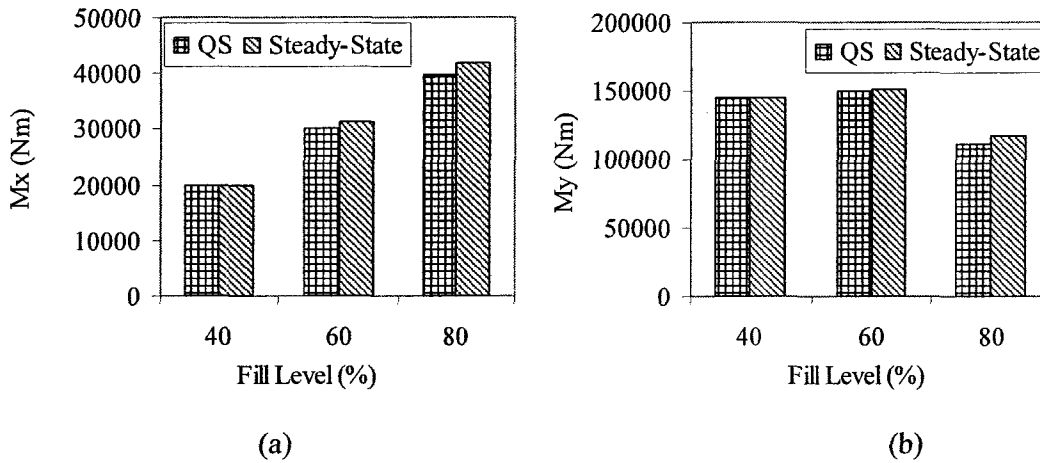


Figure 3.6: Comparisons of steady-state roll and pitch moment responses due to dynamic fluid slosh in a clean bore tank and quasi-static (QS) model responses under  $g_x = 0.3g$  and  $g_y = 0.25g$ : (a) roll moment ( $M_x$ ); and (b) pitch moment ( $M_y$ ).

The dynamic fluid slosh responses were analyzed to identify fundamental frequencies of fluid slosh in the roll and pitch planes. These frequencies are compared with those reported in the published studies to further examine the model validity. The transient lateral and longitudinal force responses obtained over the 20 s period were re-sampled at a rate of 40 Hz. The dominant frequencies of slosh forces were identified

through Fast Fourier Transform (FFT) of the time-histories with frequency resolution of 0.05 Hz. The analyses revealed fundamental slosh frequencies in the pitch plane of 0.15, 0.20 and 0.26 Hz under fill conditions of 40, 60 and 80%, respectively. These frequencies compare very well with those reported by Abramson [16] for a cylindrical tank with flat end caps (0.16, 0.21 and 0.26 Hz). The fundamental slosh frequencies in the roll plane were obtained as 0.56, 0.61 and 0.74 Hz for the 40, 60 and 80% fill levels, respectively. Which were also quite comparable with those reported by Budiansky [14] and Abramson [16] (0.56, 0.62 and 0.74 Hz). The results suggest that the curved end caps considered in this study have only slight effect on the slosh frequencies in the roll and pitch planes. The comparisons, however, suggest very good agreements between the slosh frequencies derived from the dynamic fluid slosh model with those reported in the published studies.

### **3.6 DYNAMIC FLUID SLOSH FORCES AND MOMENTS**

The dynamic slosh force and moment responses of selected configurations, derived under lateral, longitudinal and combined acceleration excitations are presented and discussed in the following subsections.

#### **3.6.1 Responses to lateral acceleration**

The transverse baffles are mostly ineffective under lateral acceleration excitation arising from steady-turn type of maneuvers. This is mostly attributed to the dominant load shift occurring in the roll plane, where baffles provide negligible resistance. The responses of selected tank configurations with 40 % fill level are thus presented in terms of lateral force ( $F_y$ ) and the roll moment ( $M_x$ ) in Figure 3.7. The figure compares the time-histories of responses to  $g_y = 0.25g$  of the clean-bore (T1) and two baffled tank

configurations (T2 and T3). The results show that the clean-bore and baffled tanks attain similar responses in the roll plane when subjected to a pure lateral excitation. The magnitudes of forces and moments were negligible in the pitch plane. Both  $F_y$  and  $M_x$  exhibit oscillations near the fundamental frequency of approximately 0.6 Hz. The peak magnitudes of  $F_y$  and  $M_x$  tend to be significantly greater than those derived from the QS solutions for the clean-bore tank. The results confirm the finding of a few recent studies that the transverse baffles are ineffective in suppressing lateral slosh [1, 2].

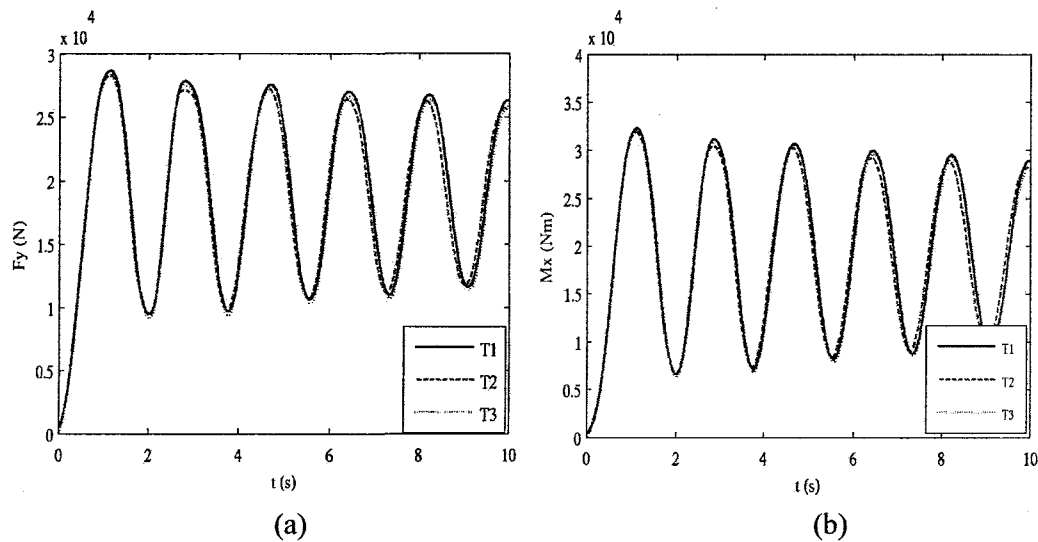


Figure 3.7: Variations in lateral slosh force and roll moment responses of 40 % filled cleanbore (T1) and baffled (T2 and T3) tanks subject to  $g_y = 0.25g$  lateral acceleration: (a) lateral force; and (b) roll moment.

### 3.6.2 Responses to longitudinal acceleration

Figure 3.8 illustrates the time histories of longitudinal slosh force and pitch moment attained for the 40% filled cleanbore (T1) and three baffled tank configurations (T2, T3 and T4) subject to  $g_x = 0.30g$ . The results suggest that fluid motion in a clean-bore tank yields considerably higher magnitudes of longitudinal slosh force and pitch moment

responses when compared to those for the baffled tanks. Further, the baffles diminish the peak moment and yield lower steady value of the pitch moment. The lower steady-state value is attributed to the transverse baffles, which cause portion of fluid to be trapped in lower section of the tank between two consecutive baffles or between the baffle and the end cap.

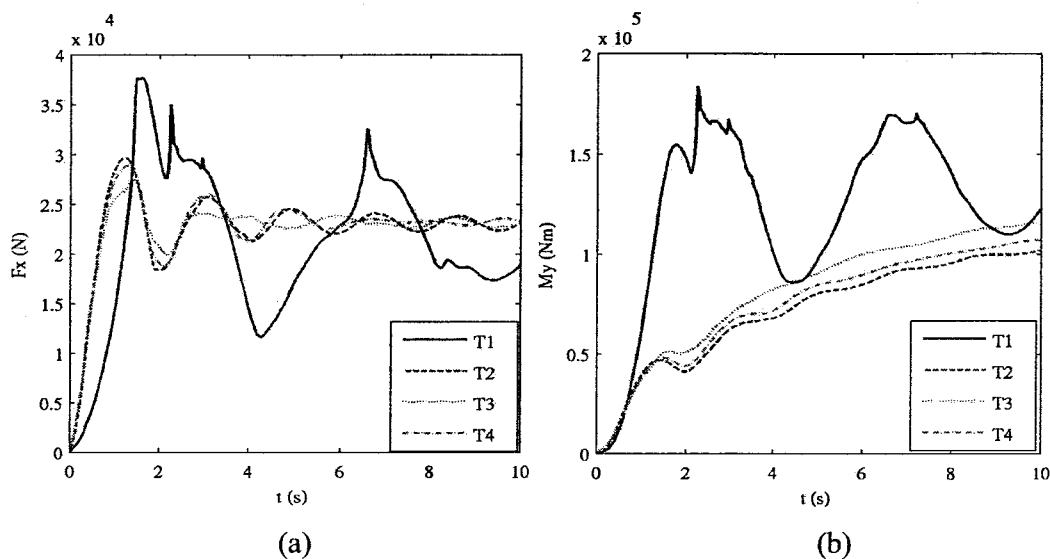


Figure 3.8: Time-histories of longitudinal slosh force and pitch moment responses of cleanbore and baffled tanks with 40 % fill level, and subject to  $g_x = 0.30g$ : (a) longitudinal slosh force; and (b) pitch moment

### 3.6.3 Responses to simultaneous longitudinal and lateral accelerations

Figure 3.9 illustrates the mean lateral and longitudinal force response of different tank configuration subject to simultaneous lateral and longitudinal excitations ( $g_x = 0.30g$  and  $g_y = 0.25g$ ) under different fill levels. The result show negligible effects of baffles on the mean lateral and longitudinal force, irrespective of the fill level. Although, it has been shown that transverse baffles are generally ineffective in

suppressing slosh in the roll plane, the results show that baffles could help reduce the magnitudes of transient lateral forces under simultaneous applications of  $g_x$  and  $g_y$ . Figure 3.10 illustrate the time histories of lateral and longitudinal slosh forces attained for the 40% filled clean-bore and baffled tanks subject to  $g_x = 0.30g$  and  $g_y = 0.25g$ . The results suggest that fluid motion in a clean-bore tank yields considerably higher magnitudes of lateral and longitudinal forces, when compared to those for the baffled tanks. The lateral slosh force oscillations for the clean-bore tank tend to diminish rapidly, while the baffled tanks responses exhibit continued oscillations of considerable magnitudes. This is attributed to the constraints imposed by the baffle walls on the fluid motion. While the peak lateral force of a clean-bore tank is only slightly higher than that of a baffled tank, the baffles tend to suppress the peak longitudinal force significantly. The results also exhibit oscillation frequencies of 0.6 and 0.2 Hz in the roll and pitch planes, respectively, which are the respective fundamental slosh frequencies. The longitudinal slosh force developed for the clean-bore tank shows continued large magnitude oscillation, as it was observed under  $g_x$  excitation alone. The responses of the baffled tanks diminish rapidly due to the flow resistance and damping effect of the baffles. The results suggest that the presence of baffles could also limit the peak lateral force under simultaneous lateral and longitudinal acceleration excitations.

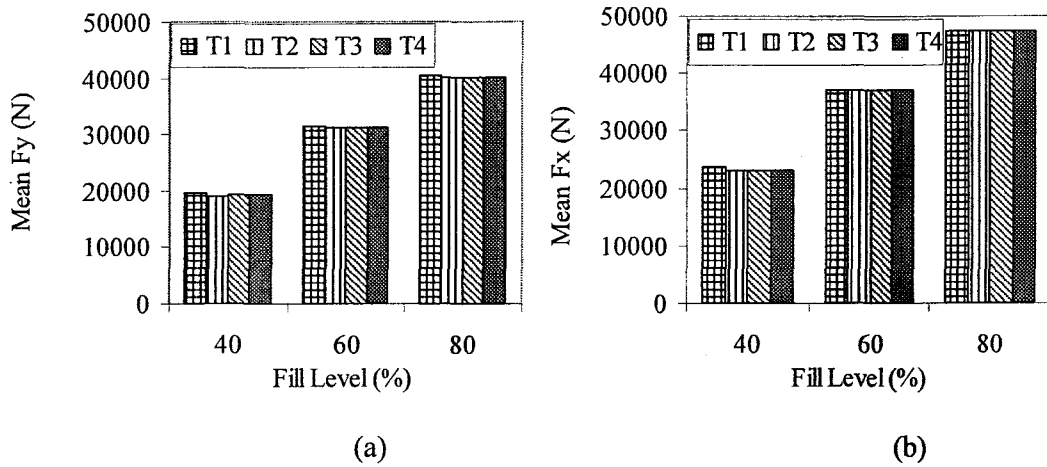


Figure 3.9: Mean lateral and longitudinal force responses of clean-bore (T1) and baffled tanks (T2, T3 and T4) with 40, 60 and 80 % fill level and subject to  $g_y = 0.25$  and  $g_x = 0.3$  g: (a) Lateral force ( $F_y$ ); and (b) Longitudinal force ( $F_x$ ).

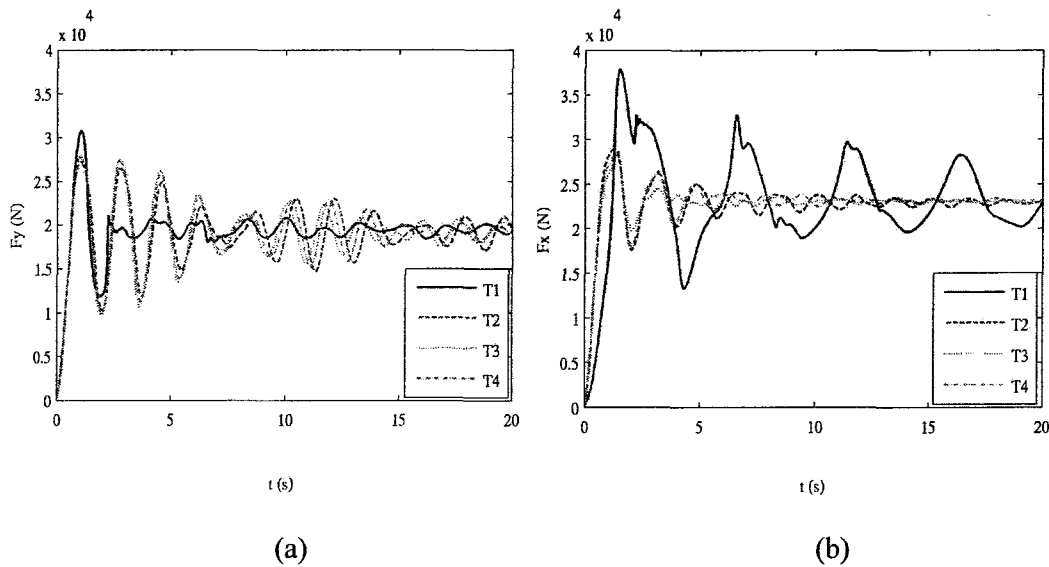


Figure 3.10: Time-histories of lateral and longitudinal slosh force responses of cleanbore and baffled tanks with 40 % fill level, and subject to  $g_y = 0.25g$  and  $g_x = 0.30g$ : (a) lateral slosh force; and (b) longitudinal slosh force.

The results further show nearly similar responses of the full baffled configurations (T2, T3 and T4) in the longitudinal direction. This may be attributed to their identical orientation along the Y-axis and opening area. The curvature and its direction with

respect to the flow, however, could affect the peak lateral force. Figure 3.11 shows the amplification factors in lateral ( $MF_y$ ) and longitudinal ( $MF_x$ ) slosh forces of different tanks with three fill levels, while subject to the same excitation. The results suggest nearly similar magnitudes of amplification factors for the full baffled configuration (T2, T3 and T4) in the longitudinal direction, while the 'T2' tank configuration attains considerably lower magnitude of amplification factor in the lateral direction, irrespective of the fill level.

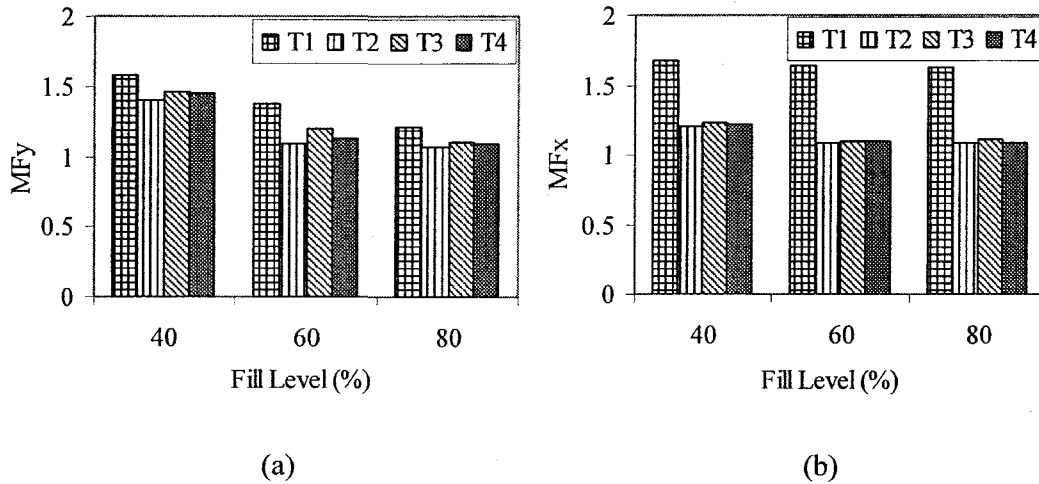


Figure 3.11: Amplification factor ( $M$ ) for lateral and longitudinal force responses of clean-bore (T1) and baffled tanks (T2, T3 and T4) with 40, 60 and 80 % fill level and subject to  $g_y = 0.25$  and  $g_x = 0.3$  g: (a) Lateral force  $M (MF_y)$ ; and (b) Longitudinal force  $M (MF_x)$ .

Figure 3.12 illustrates the time histories of roll and pitch moment responses attained for the 40% filled clean-bore (T1) and baffled tanks (T2, T3 and T4) subject to  $g_x = 0.30g$  and  $g_y = 0.25g$ . The results suggest that fluid motion in a clean-bore tank yields considerably higher magnitudes of roll and pitch moment, when compared to those for the baffled tanks. The roll moment oscillations for the clean-bore tank tend to

diminish rapidly, while the baffled tanks responses exhibit continued oscillations of considerable magnitudes, as observed for the lateral slosh force in Figure 3.10 (a). This is attributed to the constraints imposed by the baffle walls on the fluid motion. While the peak roll moment of a clean-bore tank is only slightly higher than that of a baffled tank, the presence of baffles diminishes the peak magnitude of pitch moment and yield lower steady value. The lower steady-state value is attributed to the portions of fluid trapped in lower section of the tank between two consecutive baffles or between the baffle and the end cap. Figure 3.13 shows the amplification factor in roll moment ( $MM_x$ ) of different tanks with three fill levels, while subject to the same excitation. The results suggest 'T2' tank configuration attains considerably lower magnitude of amplification factor in the roll plane, irrespective of the fill level as observed in lateral slosh force amplification factor in Figure 3.11 (a).

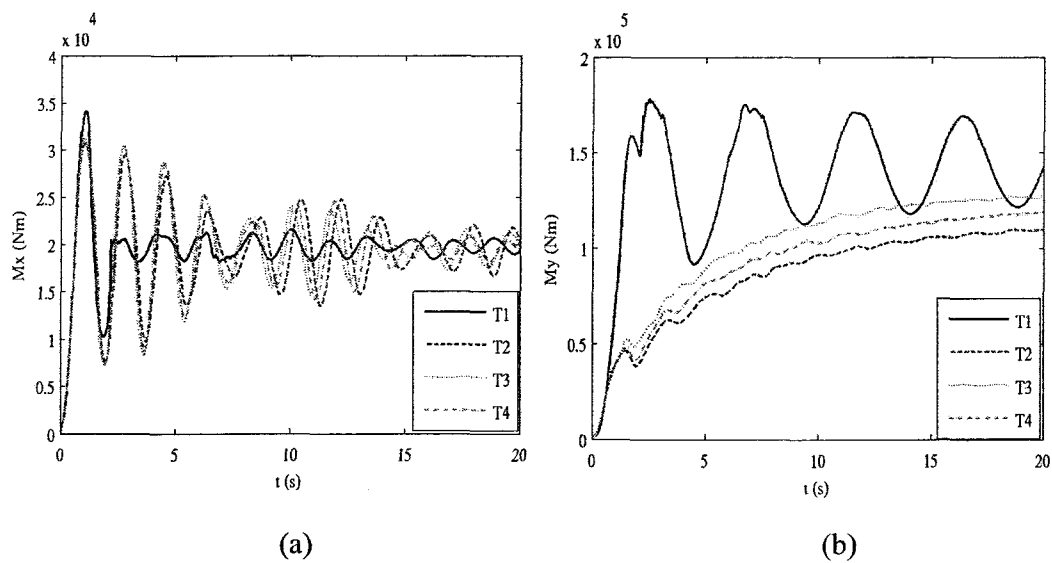


Figure 3.12: Time-histories of roll and pitch moment responses of cleanbore and baffled tanks with 40 % fill level, and subject to  $g_y = 0.25g$  and  $g_x = 0.30g$ : (a) lateral slosh force; and (b) longitudinal slosh force

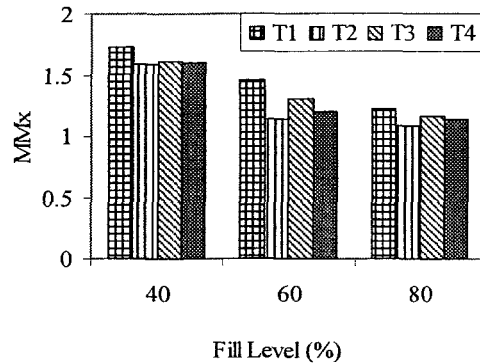


Figure 3.13: Amplification factor (M) for roll moment response of clean-bore (T1) and baffled tanks (T2, T3 and T4) with 40, 60 and 80 % fill level and subject to  $g_y=0.25$  and  $g_x=0.3$  g.

### 3.6.4 Effect of baffle opening area

The CFD models are formulated for two different orifice sizes in ‘T2’ tank configuration in order to study the effect of baffle opening. These include: (i) configuration ‘T2’ employing baffles with a small central orifice of area equal to 8% of the tank cross-section area, referred to as ‘T2a’; (ii) configuration ‘T2’ employing baffles with a large central orifice of area equal to 20% of the tank cross-section area, referred to as ‘T2b’. The selected orifice sizes are according to the CFR code, which states that a baffle opening area should not be exceed 20 % of the total tank cross section area.

Figure 3.14 shows the amplification factors in lateral ( $MF_y$ ) and longitudinal ( $MF_x$ ) slosh forces of different orifice size baffled tanks (T2a, T2 and T2b) with three fill levels, while subject to  $g_y=0.25$  and  $g_x=0.3$  g excitation. The results suggest nearly similar magnitude of amplification factor for the full orifice size baffled tank configuration (T2a, T2 and T2b) in the lateral as well as longitudinal directions, irrespective of the fill level and acceleration magnitude. The same trend has been observed in a recent study reported for optimal tank configuration [2]. The results suggest

that for the baffle orifice area less than 20% of the tank cross section area has no significant effect on the roll and pitch plane slosh forces, which is in agreement with the results reported by Propov [11] for a 2-D baffled rectangular tank. Figure 3.15 illustrate the time histories of roll and pitch moment responses attained for the 40% filled clean-bore (T1) and different orifice size baffled tanks (T2a, T2 and T2b) subject to  $g_y = 0.25$  and  $g_x = 0.3$  g excitation. The results suggest that the small orifice size baffled tank (T2a) attained considerably lower magnitude of steady-state pitch moment with considerable oscillations in the roll moment. This trend, however, is reversed for a large orifice size baffled tank (T2b). This is most likely attributed to relatively larger constraints imposed by the small orifice size baffle walls on the fluid motion.

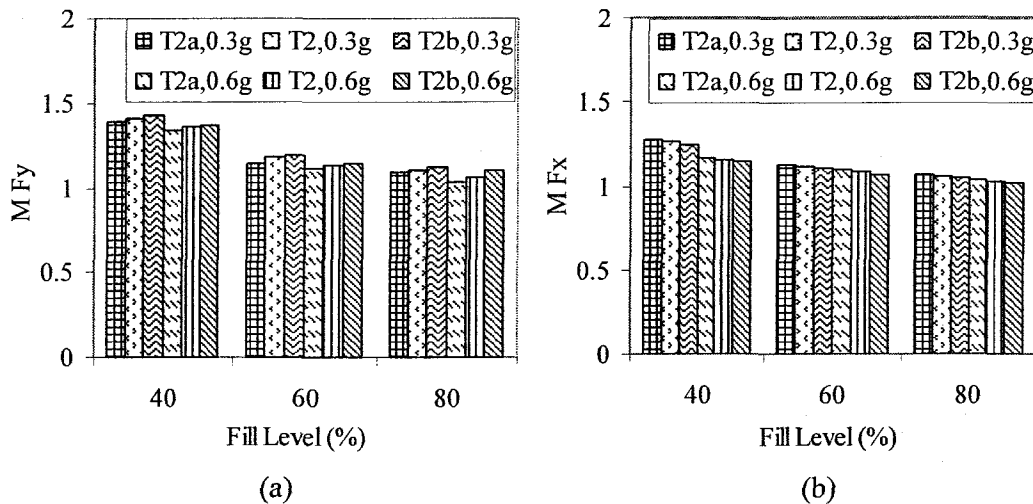


Figure 3.14: Amplification factor (M) for lateral and longitudinal force responses of different orifice size baffled tanks (T2a, T2 and T2b) with 40, 60 and 80 % fill level and subject to  $g_y = 0.25$  and  $g_x = 0.3$  ,  $g_y = 0.25$  and  $g_x = 0.6$  g : (a) Lateral force M ( $MF_y$ ); and (b) Longitudinal force M ( $MF_x$ )

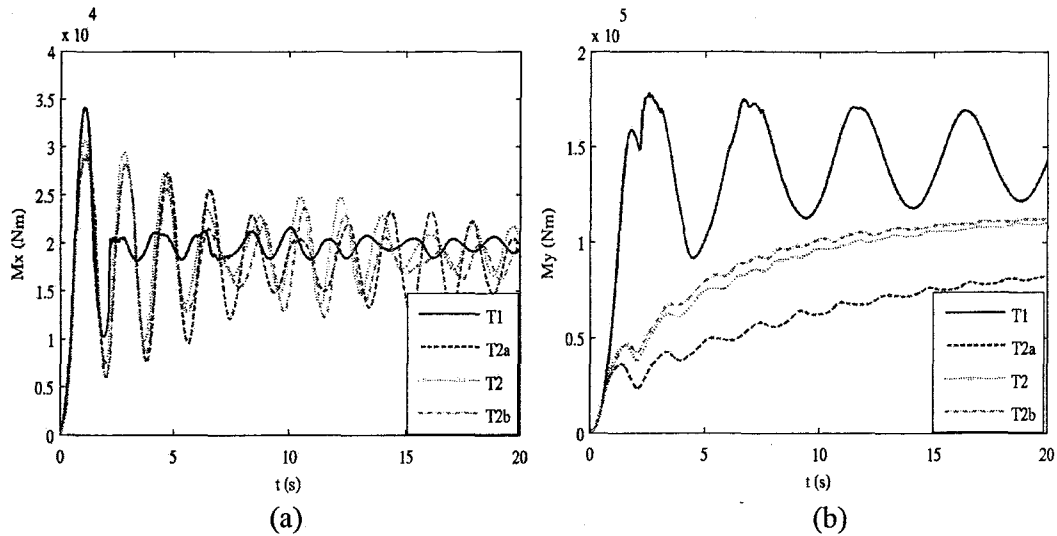


Figure 3.15: Time-histories of roll and pitch moment responses of cleanbore and various orifice size baffled tanks with 40 % fill level, and subject to  $g_y = 0.25g$  and  $g_x = 0.30g$  : (a) roll moment; and (b) pitch moment

### 3.6.5 Effect of baffle curvature depth

The CFD model is further formulated for tank configuration ‘T2’ employing baffles with a larger baffle depth of curvature (0.55m), referred to as ‘T2c’ (Figure 3.16). Figure 3.17 shows the amplification factors in lateral ( $MF_y$ ) and longitudinal ( $MF_x$ ) slosh forces, and roll moment ( $MM_x$ ) responses of different curvature depth baffled tanks (T2 and T2c) with three fill levels, while subject to  $g_y = 0.25$  and  $g_x = 0.3$  g excitation. The results suggest nearly similar magnitudes of amplification factors for both baffle depths (T2 and T2c) in the lateral as well as longitudinal direction, irrespective of the fill level. Figure 3.18 further illustrate variations in the roll and pitch moment responses of the 40% filled tank with two different baffle curvature. The results suggest that the baffle curvature depth has negligible effect on the pitch moment and very slight effect on the transient roll moment.

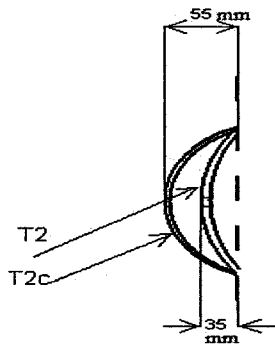


Figure 3.16: Curvature depths of single orifice full baffles ('T2' and 'T2c' tank configurations).

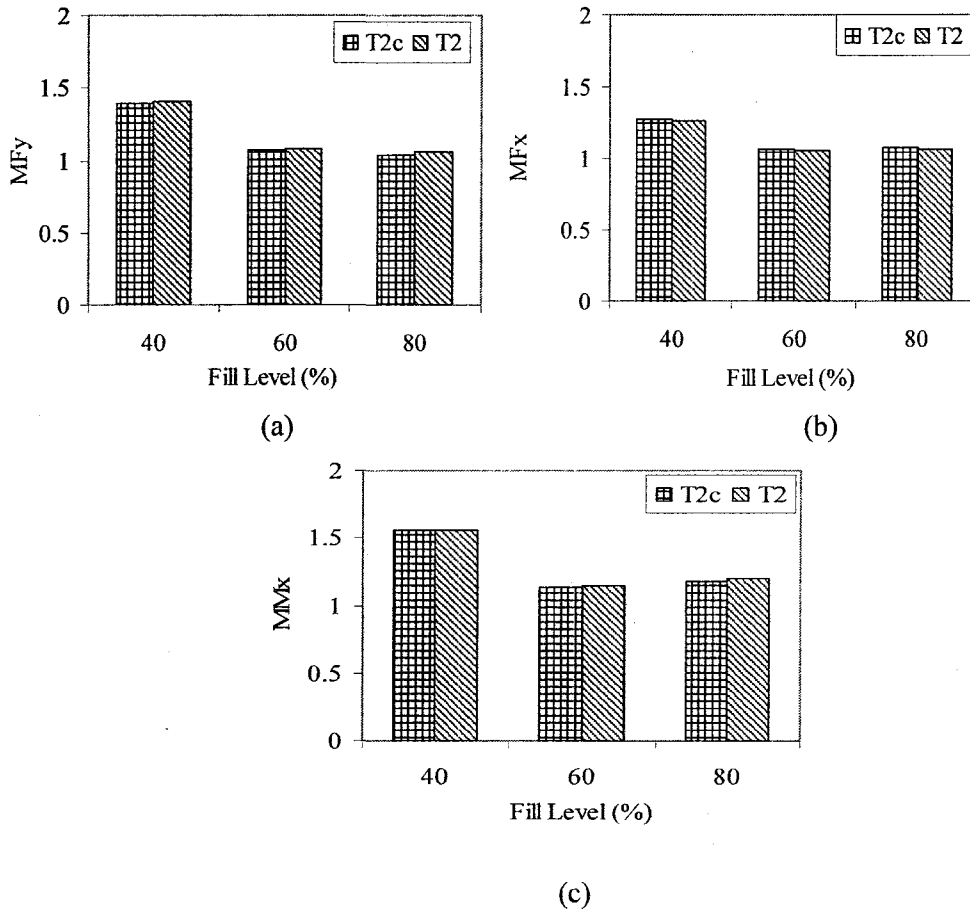


Figure 3.17: Amplification factors in lateral and longitudinal force, and roll moment responses of different curvature depth baffled tanks (T2c and T2) with 40, 60 and 80 % fill level and subject to  $g_y = 0.25$  and  $g_x = 0.3$  g: (a) Lateral force ( $MF_y$ ); (b) Longitudinal force ( $MF_x$ ); and (c) Roll moment ( $MM_x$ )

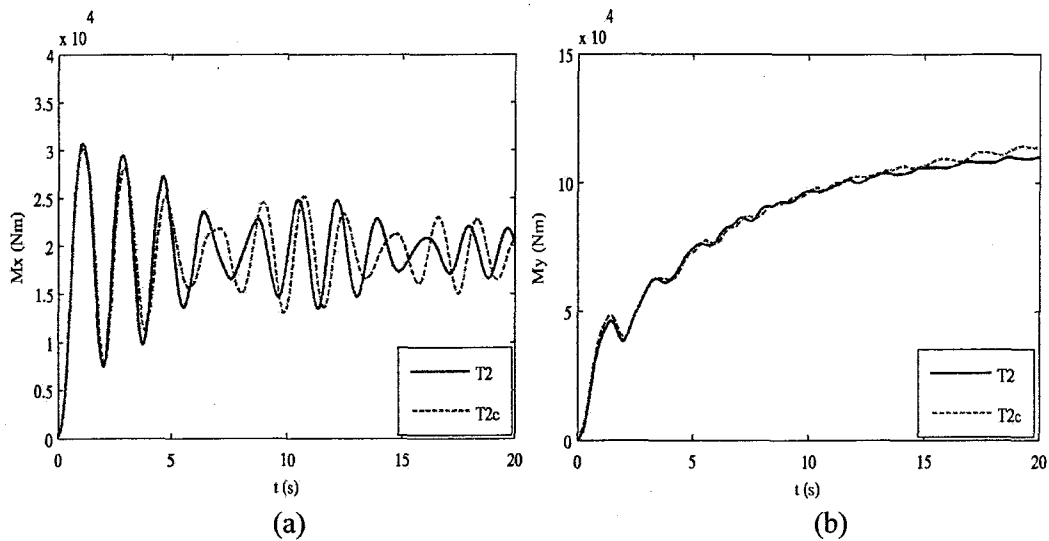


Figure 3.18: Time-histories of roll and pitch moment responses of different baffle depth tanks with 40 % fill level, and subject to  $g_y = 0.25g$  and  $g_x = 0.30g$  : (a) roll moment; and (b) pitch moment

### 3.6.6 Effect of orifice design

To seek the possibility of more effective slosh suppression for the low, intermediate and high fill levels, the orifice of the baffles are designed to be semi circular shape (tank configuration 'T5', Figure 3.2(e)). The solid upper portion of such a baffle could resist the liquid slosh in the longitudinal direction, particularly under higher fill volumes and thus yield greater effectiveness in limiting the longitudinal slosh. Figure 3.19 illustrates the time histories of lateral and longitudinal slosh forces attained for the 40% filled conventional lateral baffled (T2) and half-circle orifice baffled (T5) tanks subject to  $g_x = 0.30g$  and  $g_y = 0.25g$ . The results suggest that fluid motion in both the tank yields comparable magnitudes of lateral and longitudinal slosh force, while the responses of the 'T5' configuration tend to converge to relatively lower steady-state values.

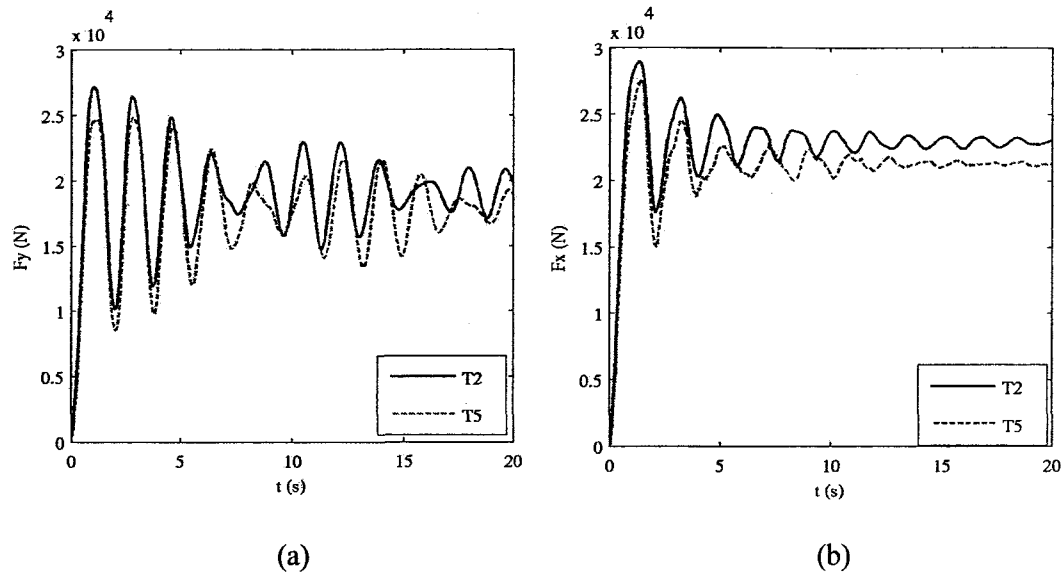


Figure 3.19: Time-histories of lateral and longitudinal slosh force responses of different orifice shape baffled tanks with 40 % fill level, and subject to  $g_y = 0.25g$  and  $g_x = 0.30g$  : (a) lateral slosh force; and (b) longitudinal slosh force

Figures 3.20 and 3.21 illustrates the time histories of roll and pitch moment responses, respectively, attained for the 40,60 and 80% filled ‘T2’ and ‘T5’ tank configurations subject to  $g_y = 0.25$  and  $g_x = 0.3 g$  excitation. The results suggest that both the tanks yield comparable magnitudes of roll and pitch moment for the low fill level (40%). Further, semi-circular orifice baffle (tank configuration ‘T5’) attains significantly higher peak roll moment than ‘T2’ tank for intermediate (60%) and high (80%) fill levels. This is attributed to relatively lower load shift in longitudinal direction through semi-circular orifice with higher load shift in lateral direction for intermediate and higher fill levels. Further results suggest that the steady-state pitch moment magnitude of a ‘T5’ tank is only slightly lower than that of a ‘T1’ tank at lower fill level (40%), this trend, however, is reversed for higher fill level (80%). Further the semi circular baffles tend to suppress the steady-state pitch moment magnitude significantly at intermediate fill level

(60%), 'T5' tank configuration attains the steady-state pitch moment almost 50% lower than that of a 'T1' tank at intermediate fill level.

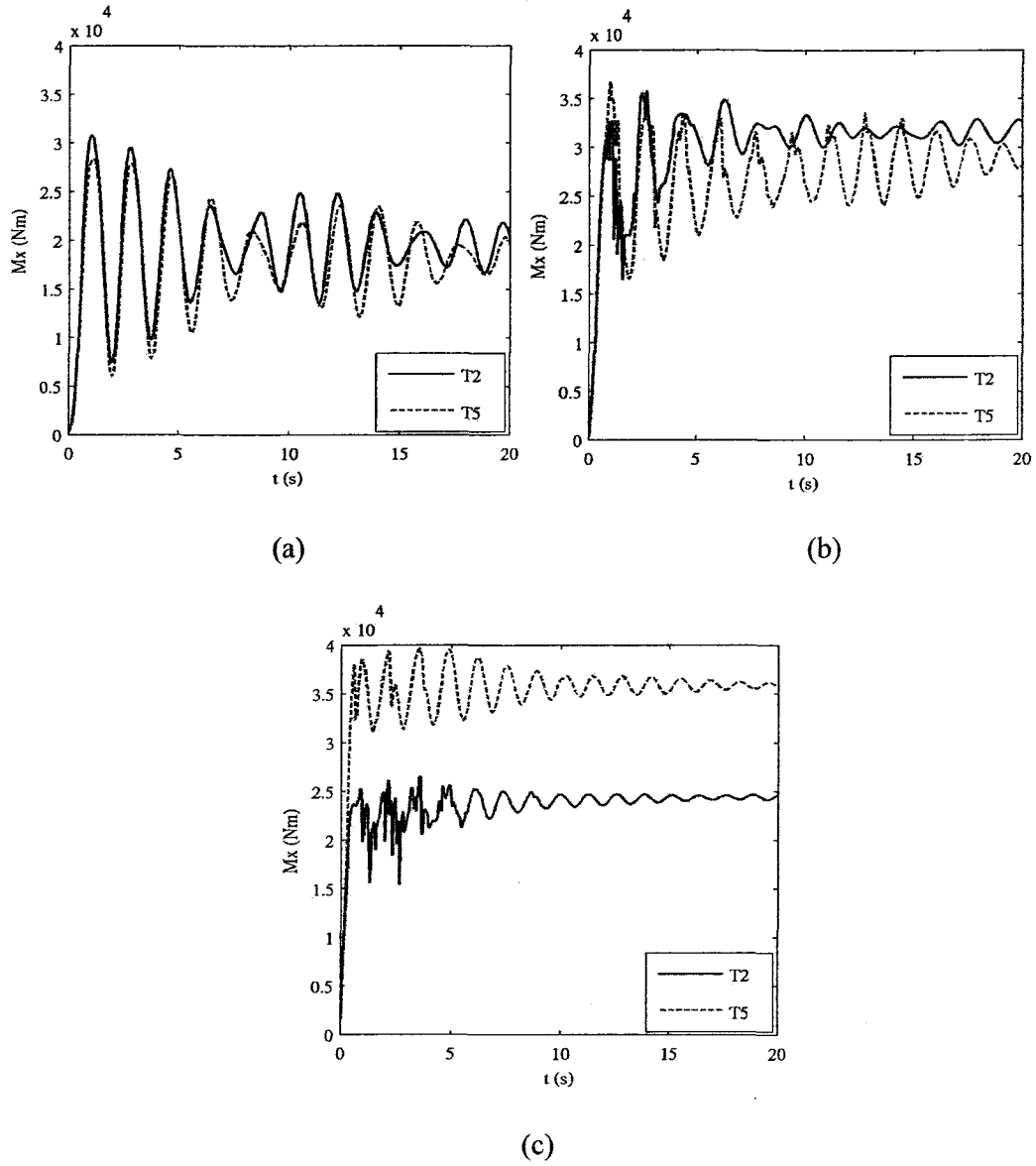


Figure 3.20: Time-histories of roll moment responses of different orifice shape baffled tanks subject to  $g_y = 0.25g$  and  $g_x = 0.30g$  : (a) 40 % fill level; (b) 60 % fill level; (c) 80 % fill level

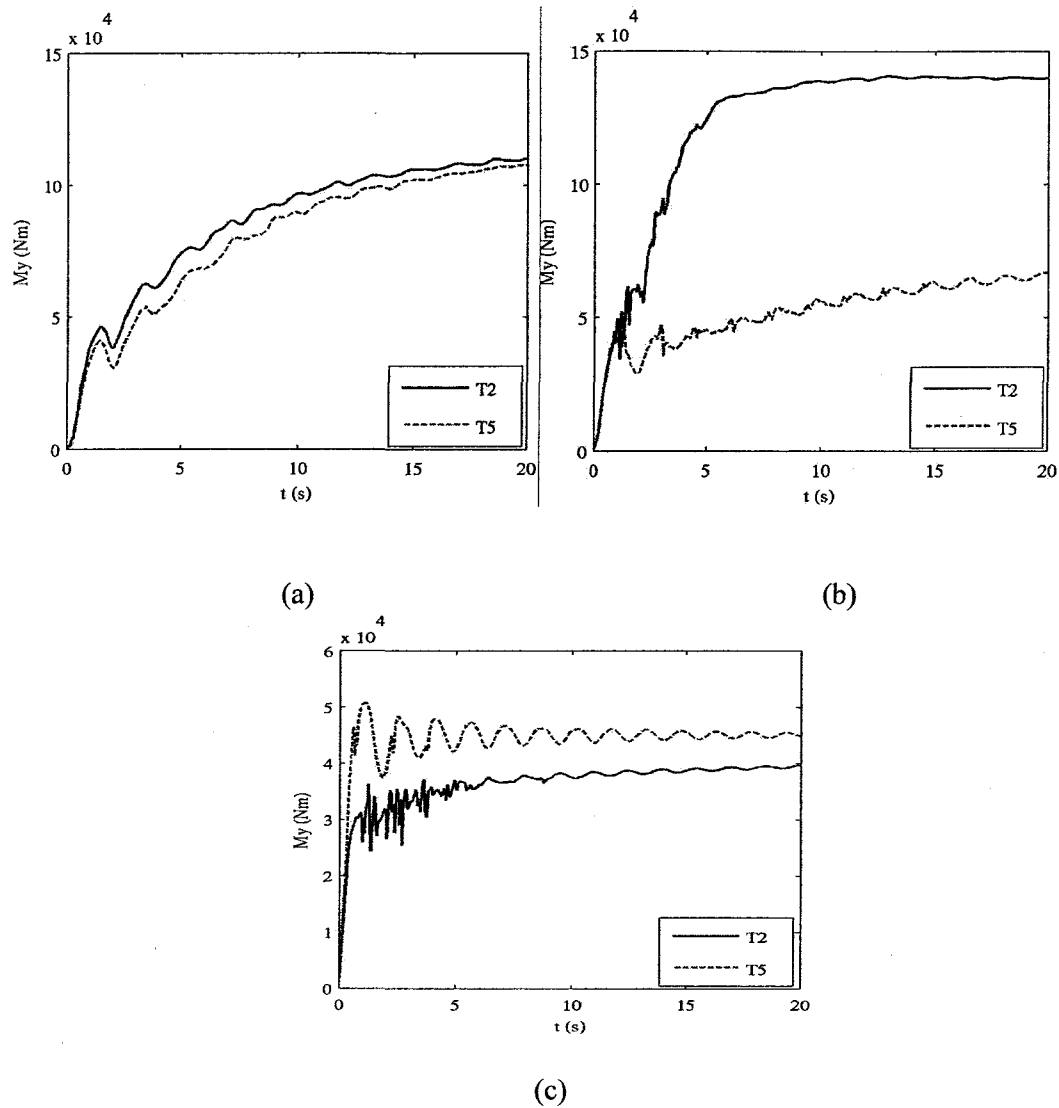


Figure 3.21: Time-histories of pitch moment responses of different orifice shape baffled tanks subject to  $g_y = 0.25g$  and  $g_x = 0.30g$ : (a) 40 % fill level; (b) 60 % fill level; (c) 80 % fill level

The non asymptotical trend and oscillation about steady value for transient pitch moment response in ‘T5’ tank configuration at high fill level indicated that with this semi circular baffles design, very little liquid cargo shifts between the baffled compartments. Figure 3.22 illustrate the visualization of the liquid free surface patterns for ‘T2’ and ‘T5’

tank configurations. The Figures show that the liquid tends to be accumulating towards the front end of the tank while the accumulation is significantly more in 'T2' tank and the free surfaces are uniform in all baffled compartments of 'T5' tank at intermediate fill level. This indicate the top half solid part can yield highly effective resistance to the fluid slosh motion when the fluid fill level little bit above the orifice.

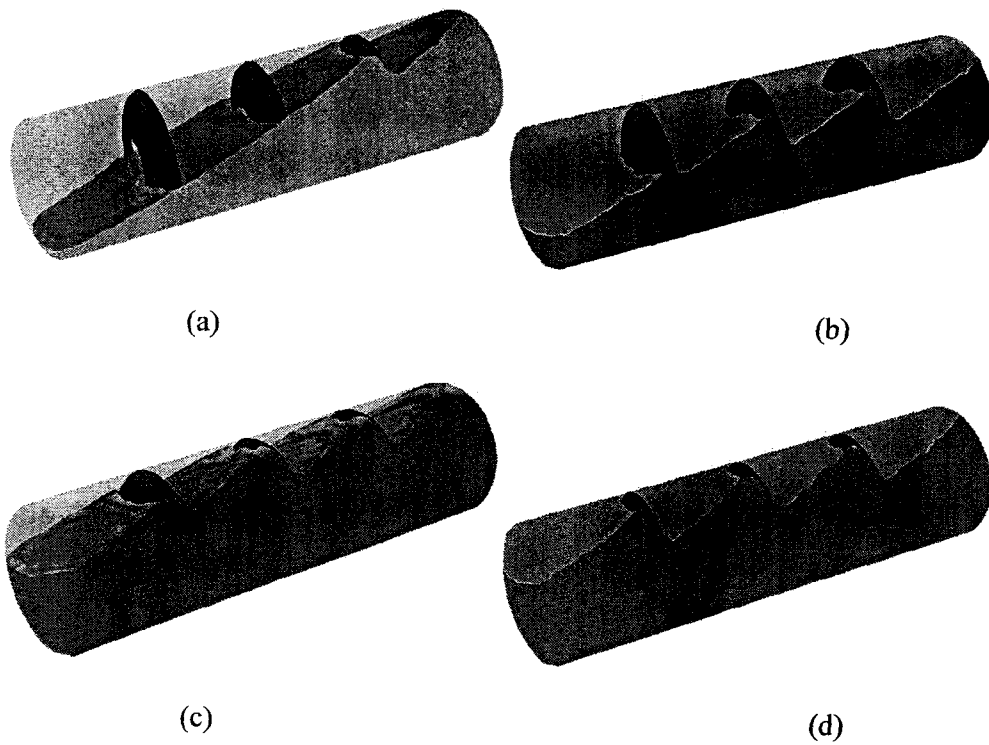


Figure 3.22: Comparison of free surface position of liquid cargo in tanks with 0.25 g and 0.3g excitation at 20 sec: (a) 60 % fill level for 'T2'; (b) 60 % fill level for 'T5'; (c) 80 % fill level for 'T2'; and (d) 80% fill level for 'T5'.

### 3.7 SUMMARY

The effect of baffle design factors on fluid slosh behavior has been analyzed within a partially filled circular cross section tank. The slosh characteristics were analyzed in terms of instantaneous cg coordinates, slosh forces and moments for different tank configuration, different fill levels and different excitations. The results suggest that the peak slosh force and moment responses in the pitch plane could be considerably suppressed through addition of the lateral baffles. Lateral slosh force and roll moment responses for the cleanbore tank, however, diminishes rapidly, while the response for the baffled tank shows continued oscillations of considerable magnitudes under simultaneous lateral and longitudinal excitations. It was also shown that the baffles curved shape almost ineffective in the roll plane when tank subject to lateral excitation, but they cause a significant influence on the pitch plane when tank subject to simultaneous lateral and longitudinal excitations. Further results revealed that the baffle orifice area less than 20% of the tank cross section area has insignificant effect on the slosh force responses, but small orifice baffles tend to yield a lower pitch moment while shows continuous oscillation in roll moment. The effects of baffle curvature depth size on fluid slosh almost negligible in both roll and pitch plane. The single half-circle orifice baffle, due to the lower orifice position and horizontal upper orifice edge, demonstrated their highly effective anti slosh role in reducing the transient pitch moments as compared to the full circle orifice baffles. The slosh suppression effect is more evident at the intermediate fill levels. The analysis also showed that high anti slosh effect achieved when orifice is fully immersed in the liquid. So the baffle orifice shape and location are important factors in improving the effectiveness of baffle to suppress the fluid slosh.

## CHAPTER 4

### TRANSIENT FLUID SLOSH ANALYSES OF OBLIQUE AND PARTIAL BAFFLED TANKS

#### 4.1 INTRODUCTION

Conventional transverse baffles employed in tank vehicles are known to effectively suppress fluid slosh in the longitudinal direction under braking and acceleration maneuvers. Such baffles, however, do not help in limiting the lateral fluid slosh under turning and braking-in-turn maneuvers [1, 2]. This is also evident from the responses presented in Figures 3.7 and 3.10. The magnitudes of lateral fluid slosh leading to dynamic load transfer in the roll plane are not affected by the lateral baffles. This dynamic load transfer contributes to the primary overturning moment in a significant manner [8]. The partly-filled tank vehicles are thus known to overturn at relatively lower levels of centrifugal forces compared to rigid cargo vehicles. Furthermore, the sloshing of a large amount of fluid can cause severe stresses in the tank structure [45]. Alternate designs of baffles that can limit fluid slosh in both the pitch and roll planes would be highly desirable in order to enhance the directional stability limits of the vehicle under turning, and braking and turning maneuvers.

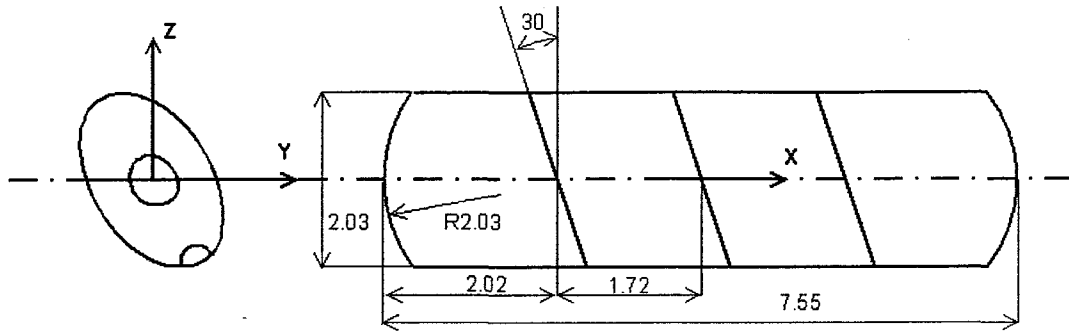
In this chapter, alternate design concepts and orientations of baffles are explored with goals of limiting both the longitudinal and lateral slosh. Concepts in obliquely placed baffles, partial baffles, and partial baffles arranged in an alternating pattern are proposed and analyzed for their effectiveness in limiting the fluid slosh. The properties of the proposed concepts are presented in terms of slosh forces and moments, and instantaneous load shifts.

## 4.2 DESIGN CONCEPTS IN OBLIQUE AND PARTIAL BAFFLES

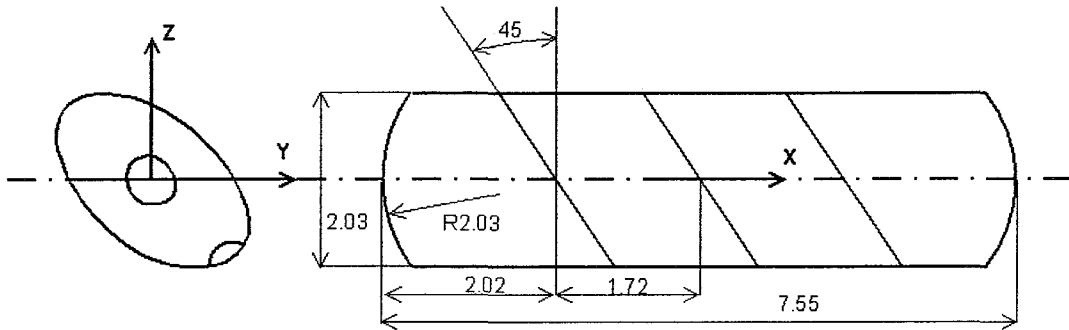
The results presented in the previous chapter suggest that the transverse baffles are generally ineffective in suppressing slosh in the roll plane. Consequently, oblique arrangements of baffles are proposed for realizing anti-slosh behavior in both the roll and pitch planes. Furthermore, a concept in partial baffle is proposed to reduce weight due to baffles. This concept is proposed considering that a relatively smaller portion of the fluid bulk undergoes excessive motion. Different arrangements of partial baffles are also proposed to achieve improved slosh suppression. The CFD models for partly-filled circular cross-section tank are formulated for six different alternate baffle configurations. These include: (i) three oblique baffles placed at 30 degrees angle with respect to the 'Z' axis, referred to as tank 'TO1' and shown in Figure 4.1(a); (ii) same as 'TO1' but baffles placed at 45 degrees angle with respect to the 'Z axis', as shown in Figure 4.1(b) and referred to as tank 'TO2'; (iii) same as 'TO1' but baffles placed at 60 degrees angle with respect to the 'Z axis', as shown in Figure 4.1(c) and referred to as tank 'TO3'; (iv) tank equipped with three half-open partial baffles placed at lower section of the tank, as shown in Figure 4.1(d) and referred to as tank 'TP1'; (v) same as 'TP1' but baffles placed at the upper section of the tank, as shown in Figure 4.1(e) and referred to as tank 'TP2'; and (vi) same as 'TP1' but baffles arranged in an alternating pattern, as shown in Figure 4.1(f) and referred to as tank 'TP3'.

The configurations 'TO1' to 'TO3' employ baffles with a flat surface and a large central orifice with opening area equal to 12% of the tank cross-section area. Each baffle is also provided with an equalizer at the bottom with total opening area being 1 % of the tank cross section area. The configurations 'TP1' to 'TP3' employ partial baffles without

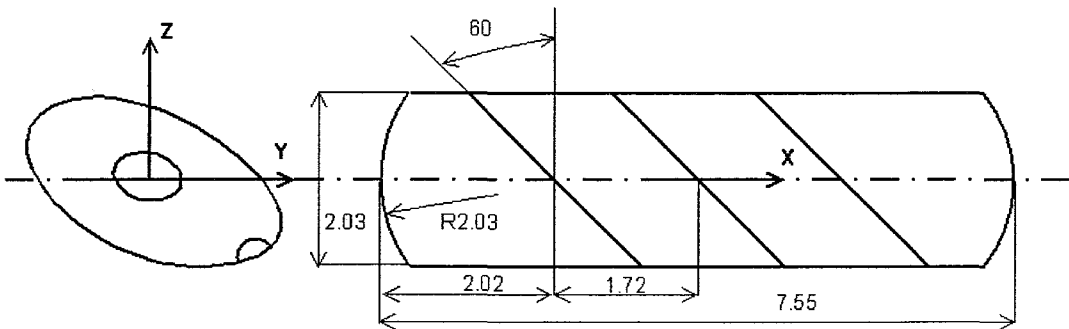
an equalizer, while the curvature of the baffles is identical to the conventional baffles illustrated for tank configuration 'T2'.



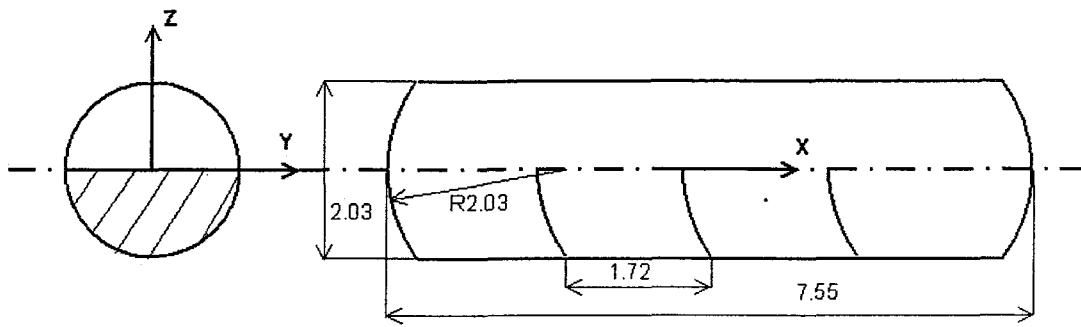
(a) Oblique baffle tank 'TO1'



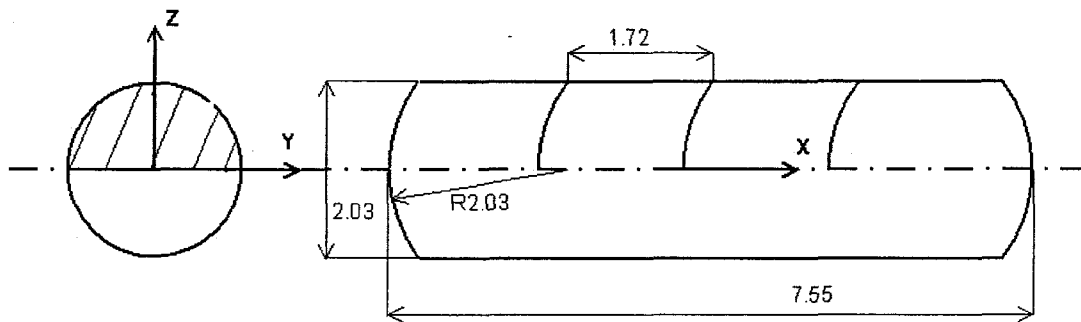
(b) Oblique baffle tank 'TO2'



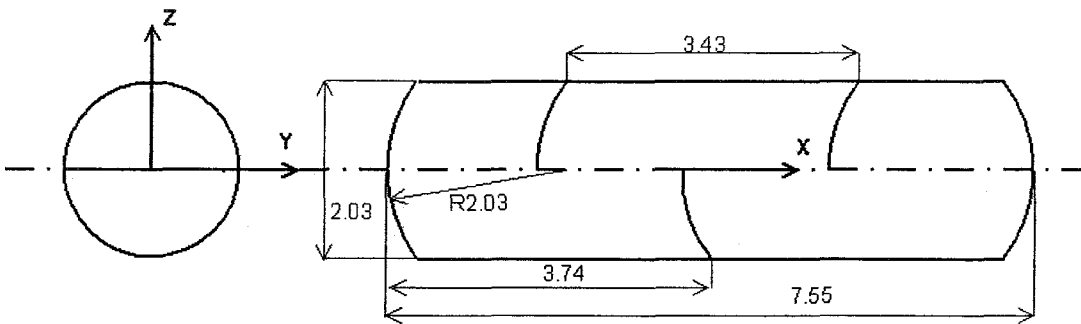
(c) Oblique baffle tank 'TO3'



(d) Half-open partial baffle tank 'TP1'



(e) Half-open partial baffle tank 'TP2'



(f) Alternate pattern of partial baffle tank 'TP3'

Figure 4.1: Schematics of the proposed baffles and their arrangements in the tank.

### **4.3 DYNAMIC FLUID SLOSH FORCES AND MOMENTS**

The CFD models of the proposed baffle and tank configurations were analyzed under the same fill levels (40, 60 and 80 %), longitudinal deceleration ( $g_x = 0.30$  and  $0.60$  g), steady turning lateral acceleration ( $g_y = 0.25$  g), and combined lateral and longitudinal acceleration during braking and turning maneuvers ( $g_y = 0.25$  and  $g_x = 0.3$  g). The tank dimensions were considered identical to the tank described in chapter 3. The dynamic slosh force and moment responses of the proposed configurations, derived under lateral, longitudinal and combined acceleration excitations, are presented and discussed in the following subsections.

#### **4.3.1 Responses of oblique baffled tanks to lateral acceleration**

The oblique baffles are mostly effective under lateral acceleration excitation arising from steady-turn type of maneuvers. This is attributed to the dominant load shift occurring in the roll plane, where oblique baffles provide significant resistance. The responses of selected tank configurations with 40 % fill level are thus presented in terms of lateral force ( $F_y$ ) and the roll moment ( $M_x$ ) in Figure 4.2. The figure compares the time-histories of responses to  $g_y = 0.25g$  of the conventional lateral baffle (T2) and three oblique baffled tank configurations (TO1, TO2 and TO3). The results suggest that fluid motion in a conventional lateral baffle tank (T2) yields considerably higher magnitudes of lateral force and roll moment, when compared to those for the oblique baffled tanks. The lateral slosh force and roll moment oscillations for the higher oblique baffled tank (TO3) tend to diminish rapidly, while the conventional lateral baffled tank (T2) responses

exhibit continued oscillations of considerable magnitudes. This is attributed to the significant resistance in roll plane by oblique baffles. These results suggest that oblique baffles with greater inclinations (TO3) are more effective in suppressing slosh in the roll plane under a lateral excitation, when compared to those for the low-angle oblique (TO1 and TO2) and conventional lateral (T2) baffled tanks.

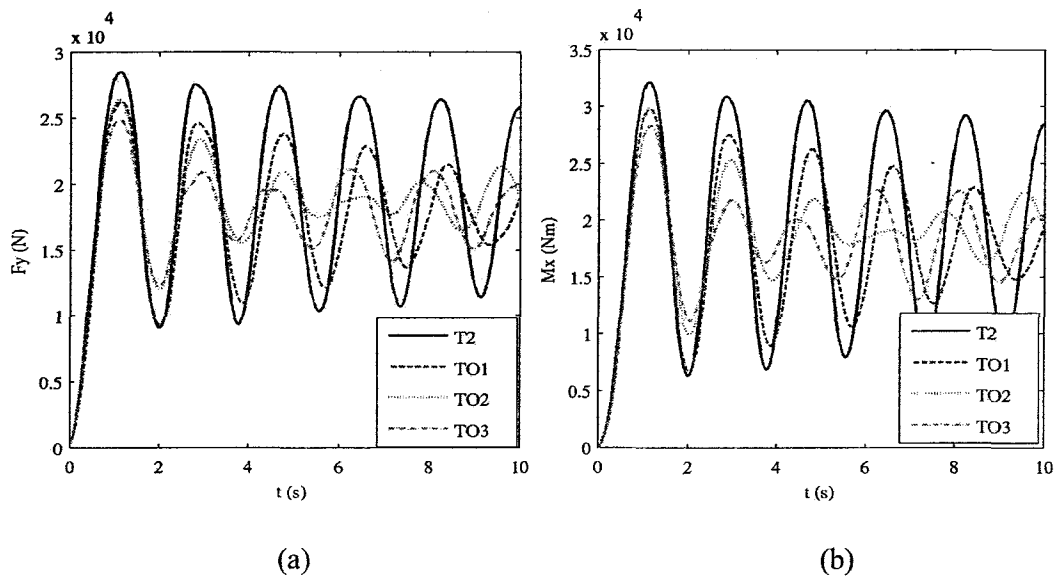


Figure 4.2: Variations in lateral slosh force and roll moment responses of 40 % filled lateral (T2) and oblique baffled (TO1, TO2 and TO3) tanks subject to  $g_y = 0.25g$  lateral acceleration: (a) lateral force; and (b) roll moment.

#### 4.3.2 Responses of oblique baffled tanks to longitudinal acceleration

Figure 4.3 illustrates the time histories of longitudinal slosh force and pitch moment attained for the 40% filled conventional lateral baffle (T2) and three oblique baffled tank configurations (TO1, TO2 and TO3) subject to  $g_x = 0.60g$ . The results suggest that fluid motion in all tanks yields comparable magnitudes of peak longitudinal force suggesting that obliquely placed baffles are as effective as the conventional lateral baffles (T2) in suppressing longitudinal slosh forces.

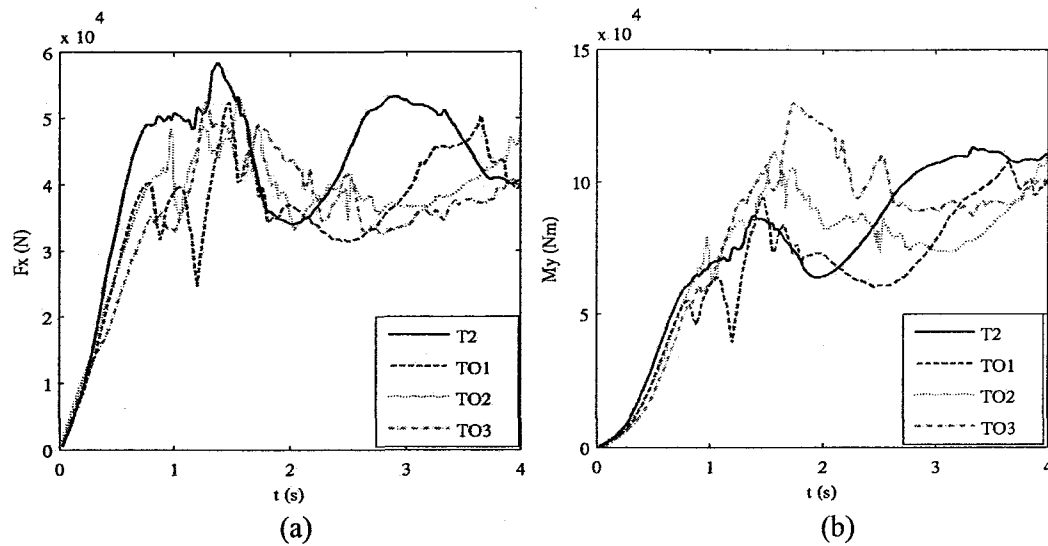


Figure 4.3: Variations in longitudinal slosh force and pitch moment responses of 40 % filled lateral (T2) and oblique baffled (TO1, TO2 and TO3) tanks subject to  $g_x = 0.60g$  longitudinal acceleration: (a) longitudinal force; and (b) pitch moment.

#### 4.3.3 Responses of oblique baffled tanks to simultaneous longitudinal and lateral accelerations.

Figure 4.4 shows the amplification factors in lateral ( $MF_y$ ) and longitudinal ( $MF_x$ ) slosh forces of conventional lateral baffle (T2) and three oblique baffled tank configurations (TO1, TO2, TO3) with the three fill levels, while subject to  $g_x = 0.30g$  and  $g_y = 0.25g$  excitations. The results suggest that the force amplification factors of the baffled tanks decrease with an increase in fill level as observed in case of the cleanbore and lateral baffled tanks. This is attributed to the proportionally larger load shift in the roll and pitch plane in the case of lower fill level. Further, nearly similar magnitudes of amplification factors for the full oblique baffled configurations (TO1, TO2 and TO3) are observed in the lateral and longitudinal directions. Figure 4.5 illustrates the time histories of lateral and longitudinal slosh force attained for the 40% filled conventional lateral baffle (T2) and three oblique baffled tank configurations (TO1, TO2 and TO3) subject to

$g_x = 0.30g$  and  $g_y = 0.25g$  excitations. The results suggest the peak lateral and longitudinal force of a conventional lateral baffled tank (T2) is only slightly higher than that of an oblique baffled tank. The lateral slosh force oscillations for the oblique baffled tank tend to diminish rapidly as observed for the clean-bore tank (T1), while the conventional lateral baffled tank (T2) response exhibits continued oscillations of considerable magnitudes. This is attributed to the oblique baffles providing considerable resistance to slosh in both roll and pitch planes. The flow visualization further illustrated delayed accumulation of liquid at the front end of the oblique baffled tank, which caused the oscillations in longitudinal force to diminish as observed for the lateral baffled tank.

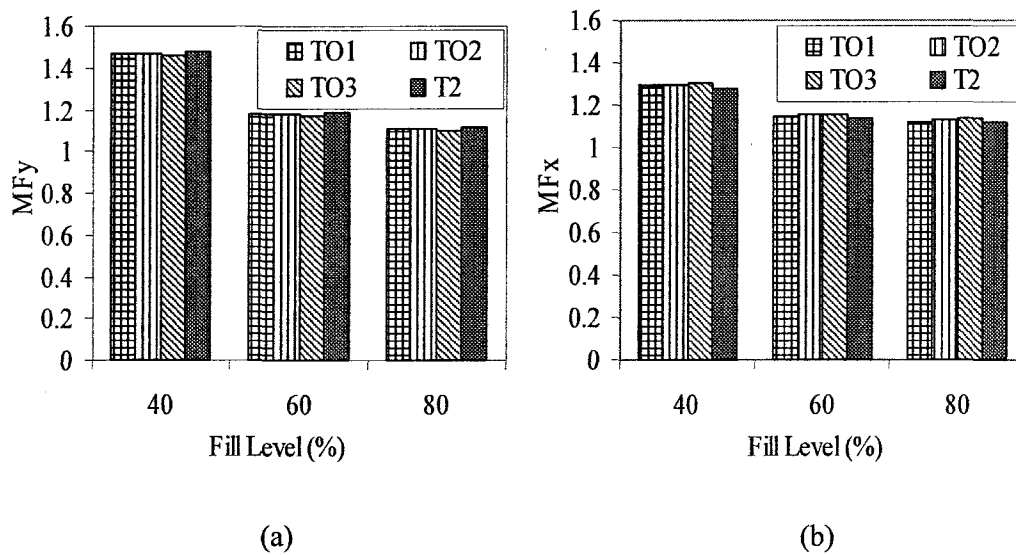


Figure 4.4: Amplification factors of lateral ( $MF_y$ ) and longitudinal ( $MF_x$ ) force responses of lateral (T2) and oblique baffled tanks (TO1, TO2 and TO3) with 40, 60 and 80 % fill level and subject to  $g_y = 0.25$  and  $g_x = 0.3$  g: (a) Lateral force ( $MF_y$ ); and (b) Longitudinal force ( $MF_x$ ).

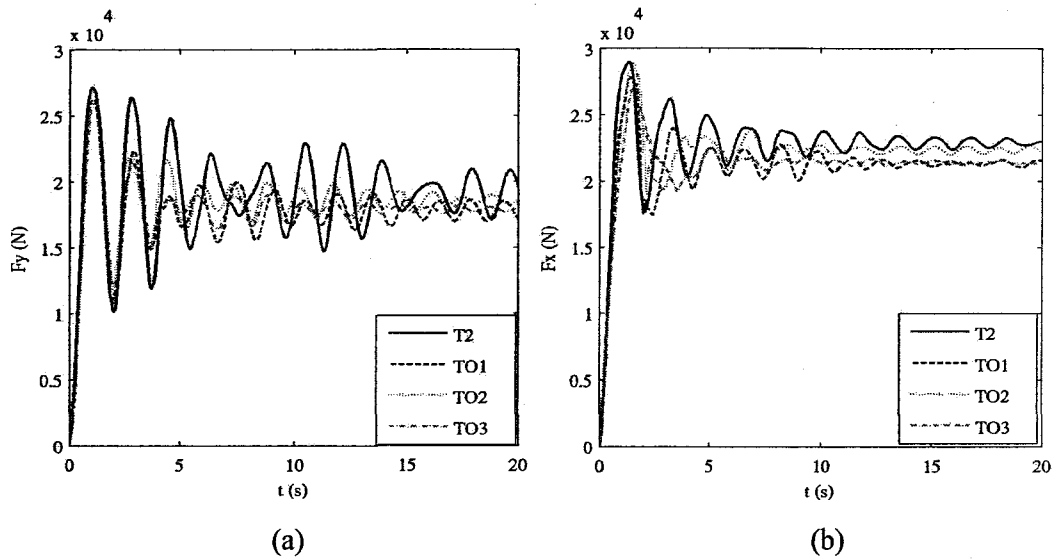


Figure 4.5: Time-histories of lateral and longitudinal slosh force responses of lateral and oblique baffled tanks with 40 % fill level, and subject to  $g_y = 0.25g$  and  $g_x = 0.30g$  : (a) lateral slosh force; and (b) longitudinal slosh force

Figure 4.6 shows the amplification factor in roll moment ( $MM_x$ ) of lateral and oblique baffled tanks with the three fill levels, while subject to the same excitation. The results suggest 'T2' tank configuration attains slightly lower magnitude of amplification factor in the roll plane when compared to those for oblique baffled tanks, irrespective of the fill level, while nearly similar magnitudes of amplification factors are obtained for the entire full oblique baffled configuration (TO1, TO2 and TO3). Figure 4.7 illustrates the time histories of roll and pitch moment responses attained for the 40% filled lateral baffled tank (T2) and oblique baffled tanks (TO1, TO2 and TO3) subject to  $g_x = 0.30g$  and  $g_y = 0.25g$ . The results suggest that the roll moment oscillations for the oblique baffled tanks tend to diminish rapidly, while the lateral baffled tank (T2) responses exhibit continued oscillations of considerable magnitudes, as observed for the lateral slosh force in Figure 4.5 (a). While the peak roll moment of an oblique baffled

tank is only slightly higher than that of a baffled tank. The pitch moment response of the TO3 configuration exhibits a higher transient peak near 1.88, while the roll moment peak of the lateral baffled tank is slightly lower than those of the oblique baffled configuration. This may be attributed to relatively lesser amount of fluid trapped in the rear section of the higher oblique baffled tank (TO3) composed to the other configurations. All the three oblique baffled configuration exhibit similar response after 2 s.

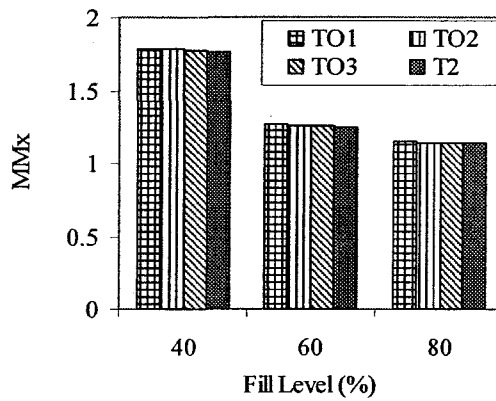


Figure 4.6: Amplification factors of roll moment ( $MM_x$ ) responses of lateral (T2) and oblique baffled tanks (TO1, TO2 and TO3) with 40, 60 and 80 % fill level and subject to  $g_y = 0.25$  and  $g_x = 0.3$  g

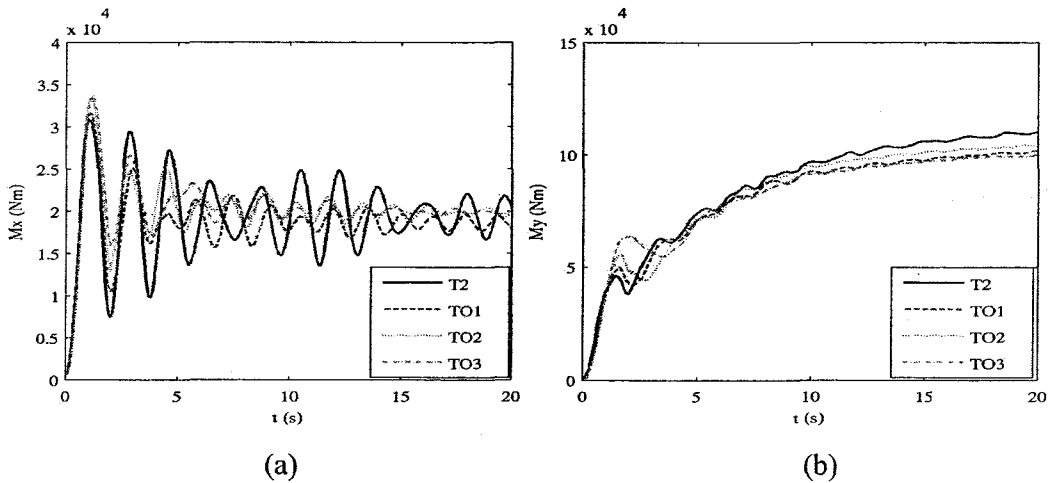


Figure 4.7: Time-histories of roll and pitch moment responses of lateral and oblique baffled tanks with 40 % fill level, and subject to  $g_y = 0.25g$  and  $g_x = 0.30g$ : (a) roll moment; and (b) pitch moment

#### 4.3.4 Responses of a partial baffled tank to lateral acceleration

The partial transverse baffles would be mostly ineffective under lateral acceleration excitation arising from steady-turn type of maneuvers, although these could provide adequate resistance to longitudinal slosh with considerable weight reduction. This is mostly attributed to the dominant load shift in the roll plane under a lateral acceleration excitation, where such baffles provide negligible resistance. The responses of selected tank configurations with 40 % fill level are thus presented in terms of lateral force ( $F_y$ ) and the roll moment ( $M_x$ ) in Figure 4.8.

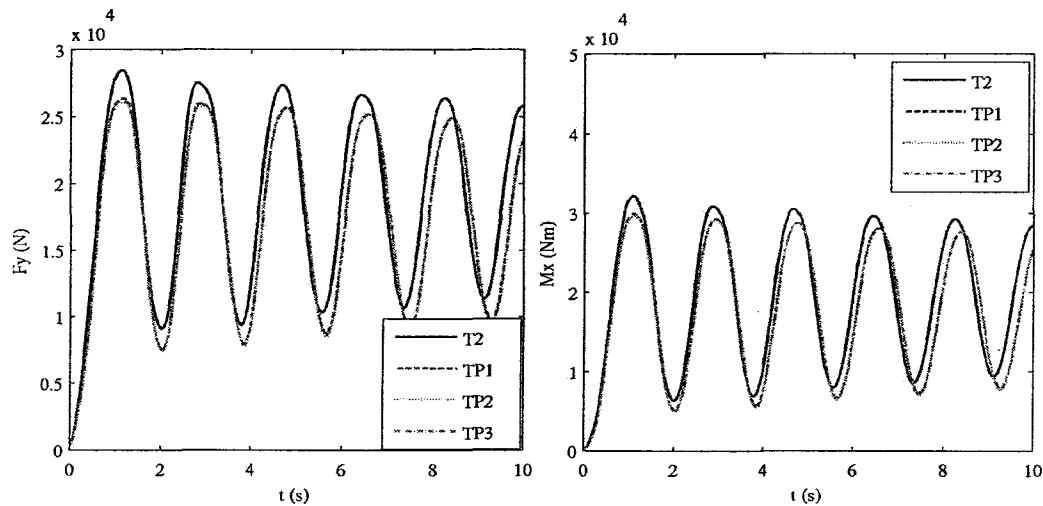


Figure 4.8: Variations in lateral slosh force and roll moment responses of 40 % filled lateral (T2) and partial baffled (TP1, TP2 and TP3) tanks subject to  $g_y = 0.25g$  lateral acceleration: (a) lateral force; and (b) roll moment.

The Figure compares the time-histories of responses to  $g_y = 0.25g$  of the lateral baffle (T2) and three partial baffled tank configurations (TP1, TP2 and TP3). The results show that the partial baffled tank configurations (TP1, TP2 and TP3) attain similar responses in the roll plane when subjected to a pure lateral acceleration excitation,

although the 'T2' tank yields relatively larger roll moment. The magnitudes of forces and moments developed in the pitch plane were very small, which revealed oscillations near the fundamental frequency of approximately 0.6 Hz.

#### **4.3.5 Responses of a partial baffled tank to a longitudinal acceleration**

The liquid slosh behavior in partly-filled partial baffled tanks (TP1, TP2 and TP3) has been analyzed with three fill levels, while subject to a pure longitudinal deceleration,  $g_x = 0.30g$ , excitation. Figure 4.9 illustrates the time histories of longitudinal slosh force attained for the 40, 60 and 80% filled conventional lateral baffle (T2) and three partial baffled tank configurations (TP1, TP2 and TP3) subject to  $g_x = 0.30g$ . The results show that the tank configurations 'TP2' with upper-half parting wall yields considerably larger longitudinal force under the lower fill level (40%), while configuration 'TP1' with lower-half partition wall yields higher longitudinal force under higher fill level (80%). Tank configuration 'TP3' with alternate partial baffles shows magnitudes of longitudinal force that are comparable to that of the lateral baffled tank (T1), irrespective of the fill level. Figure 4.10 illustrates the time histories of pitch moment attained for the 40, 60 and 80% filled conventional lateral baffle (T2) and three partial baffled tank configurations (TP1, TP2 and TP3) subject to  $g_x = 0.30g$ . The results show that the tank configuration 'TP1' suppresses the steady-state pitch moment considerably for the lower fill level (40%), while the tank configuration 'TP2' attains lower steady-state pitch moment for the medium and higher fill levels (60 and 80%). The alternate pattern of partial baffles (configuration 'TP3') yields considerably lower steady-state pitch moment, irrespective of the fill level.

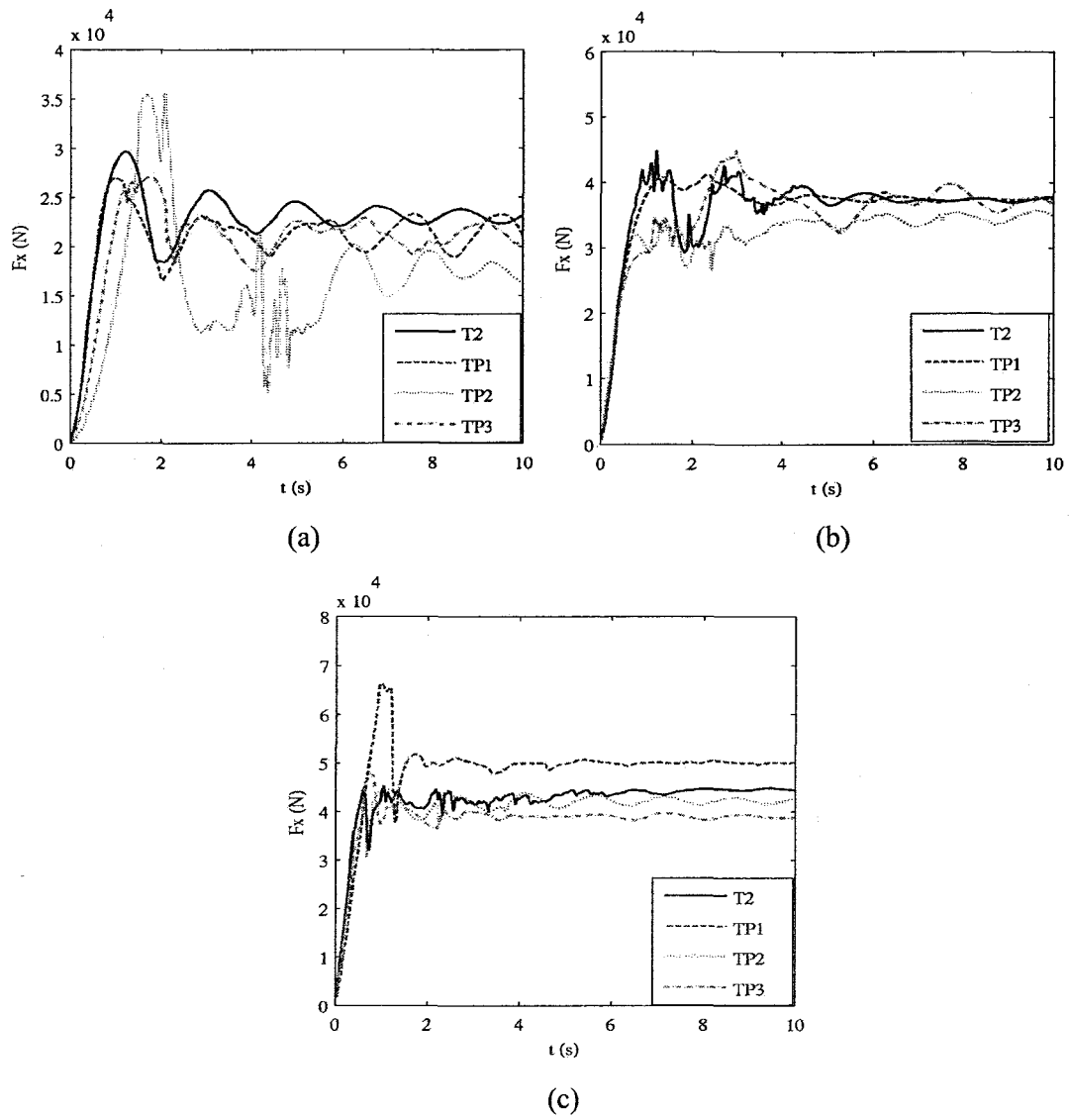
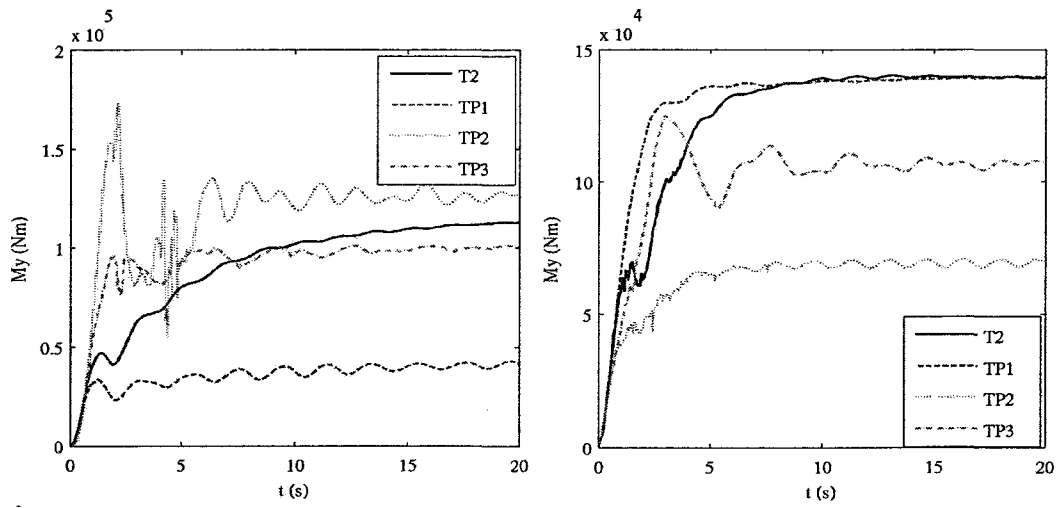
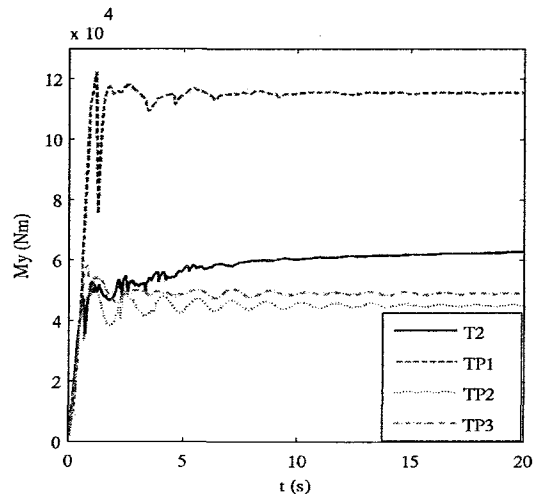


Figure 4.9: Time-histories of longitudinal force responses of lateral and partial baffled tanks subject to  $g_x = 0.30g$  : (a) 40 % fill level; (b) 60 % fill level; (c) 80 % fill level



(a)

(b)



(c)

Figure 4.10: Time-histories of pitch moment responses of lateral and partial baffled tanks subject to  $g_x = 0.30g$  : (a) 40 % fill level; (b) 60 % fill level; (c) 80 % fill level

### 4.3.6 Responses of partial baffled tank configurations to simultaneous longitudinal and lateral accelerations

Figure 4.11 illustrates the time histories of lateral and longitudinal slosh force responses attained for the 40% filled conventional lateral baffle (T2) and three partial baffled tank configurations (TP1, TP2 and TP3) subject to  $g_x = 0.30g$  and  $g_y = 0.25g$ . The results suggest that the peak lateral force of the 'TP2' tank is only slightly higher than that of other baffled tanks, while the bottom partial baffles (TP1) tend to suppress the peak longitudinal force significantly for the 40 % fill level. The 'TP1' configuration, however, yields considerably higher peak longitudinal force.

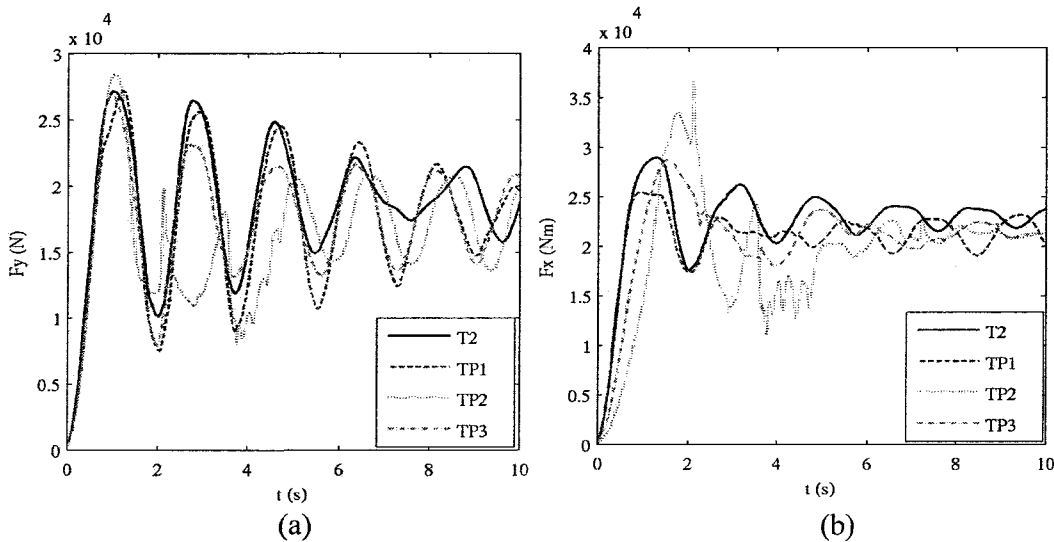
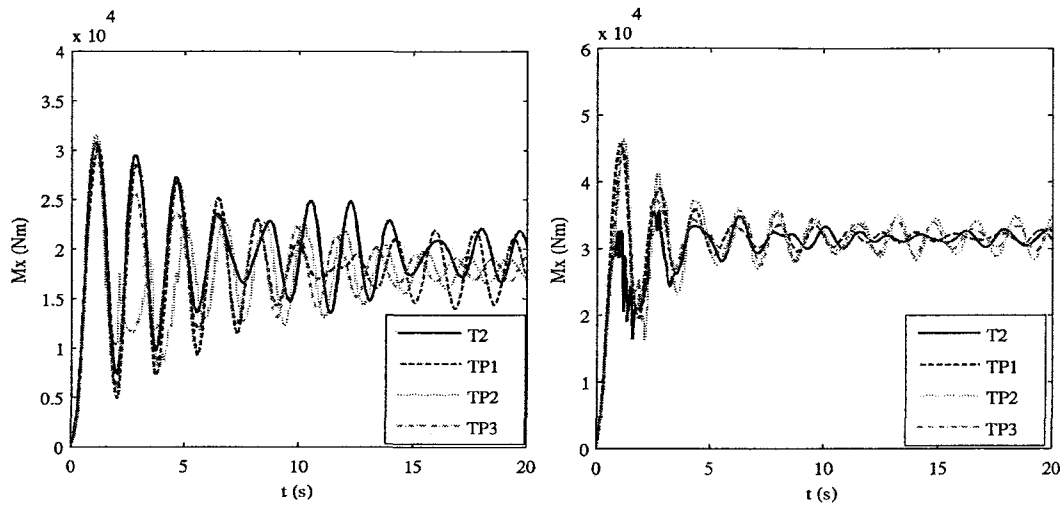


Figure 4.11: Time-histories of lateral and longitudinal slosh force responses of lateral and partial baffled tanks with 40 % fill level, and subject to  $g_y = 0.25g$  and  $g_x = 0.30g$ : (a) lateral slosh force; and (b) longitudinal slosh force

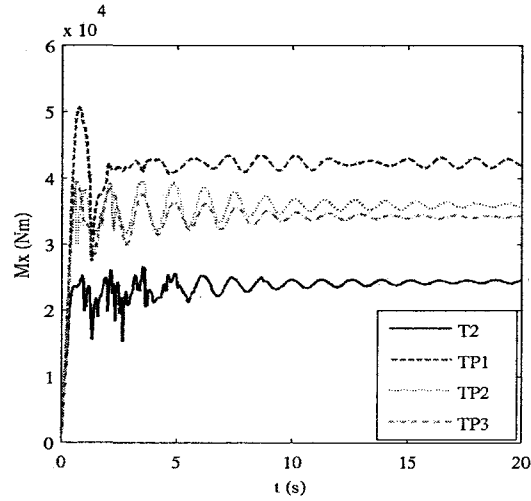
Figure 4.12 illustrates the time histories of roll moment attained for the 40, 60 and 80% filled conventional lateral baffle (T2) and three partial baffled tank configurations (TP1, TP2 and TP3) subject to  $g_x = 0.30g$  and  $g_y = 0.25g$  excitations. The results suggest that oscillations in roll moment response of the 'TP2' tank tend to diminish rapidly as

observed in case of the clean-bore tank (T1), while the lateral baffled tank (T2) responses exhibit continued oscillations of considerable magnitudes for the lower fill level (40%). This is attributed to the negligible flow resistance offered by the upper partial baffles under lower fill level. While the peak roll moment response of the lateral baffled tank (T2) is almost similar to that of partial baffled tanks (TP1, TP2 and TP3) for the lower fill level (40%), the lateral baffles (T2) yield lower peak roll moment significantly under medium and higher fill levels (60 and 80 %). This is attributed to lower lateral load shift in the 'T2' tank compared to the partial tank configurations (TP1, TP2 and TP3). The full baffles tend to trap greater amount of fluid in compartments and between the tank than partial baffled tanks. Figure 4.13 illustrates the time histories of pitch moment attained for the 40, 60 and 80% filled conventional lateral baffle (T2) and three partial baffled tank configurations (TP1, TP2 and TP3) subject to  $g_x = 0.30g$  and  $g_y = 0.25g$  excitations. The results shows that, tank configurations 'TP1', 'TP2' and 'T2' attain considerably lower steady-state pitch moment magnitude for the 40, 60 and 80 % fill levels, respectively. The configuration 'TP3', however, diminishes the steady-state pitch moment magnitude considerably, irrespective of the fill levels. The tank configuration 'TP2' and 'TP1' attain high peak pitch moment for 40 and 80 % fill levels, respectively. This is attributed to the tank configuration 'TP1' baffles fully merged in the fluid for the higher fill level (80 %), while the configuration 'TP2' baffles offer negligible resistance to fluid motion for the lower fill level (40 %).



(a)

(b)



(c)

Figure 4.12: Time-histories of the roll moment responses of lateral and partial baffled tanks subject  $g_y = 0.25g$  and  $g_x = 0.30g$ : (a) 40 % fill level; (b) 60 % fill level; (c) 80 % fill level

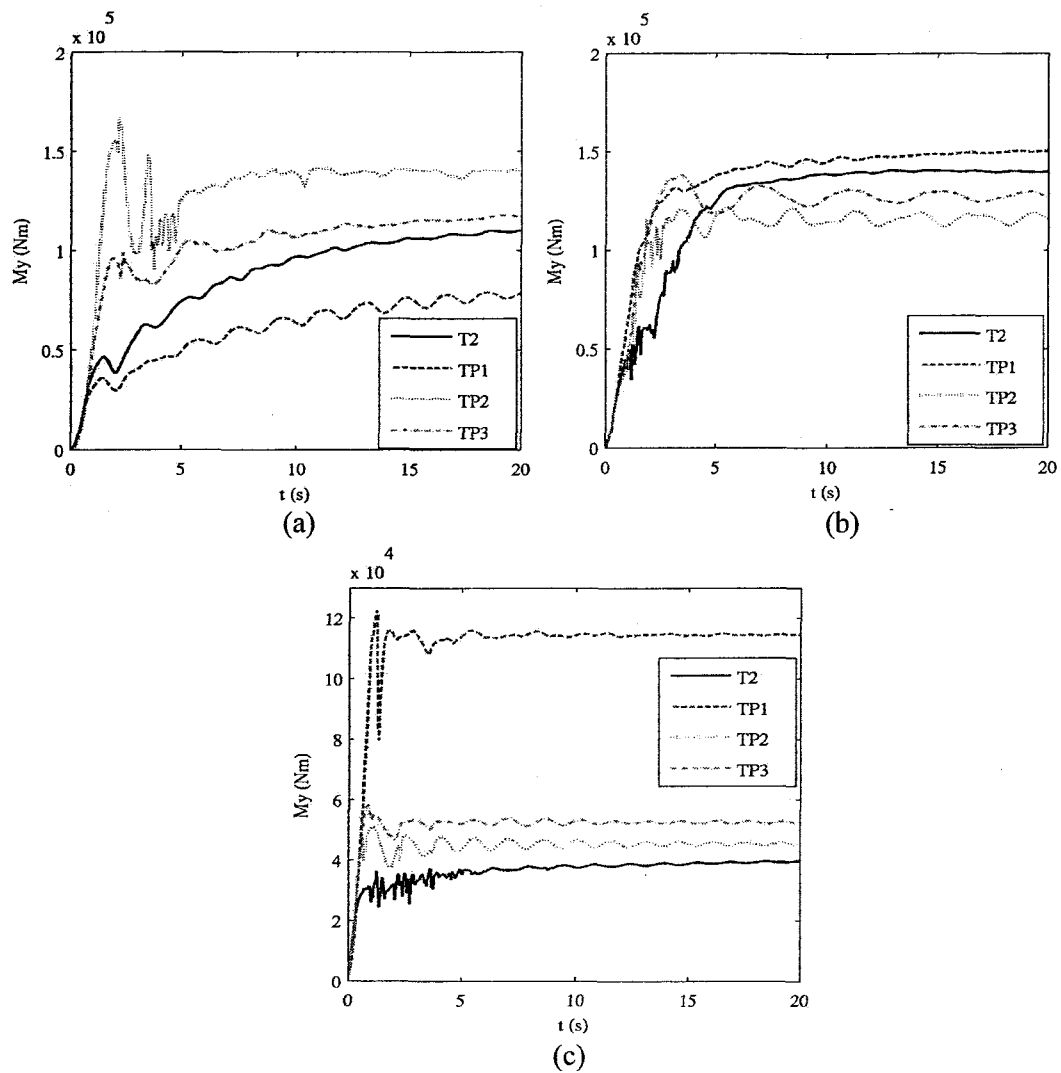


Figure 4.13: Time-histories of the pitch moment responses of lateral and partial baffled tanks subject  $g_y = 0.25g$  and  $g_x = 0.30g$  : (a) 40 % fill level; (b) 60 % fill level; (c) 80 % fill level

#### 4.4 SUMMARY

Concepts in different oblique and partial baffles are proposed to minimize the dynamic slosh force in the pitch and roll planes. The effects of proposed baffle designs concept on the fluid slosh behavior have been analyzed within a partially filled circular cross section tank. The slosh characteristics of the proposed concepts were compared with those of conventional lateral baffled tank. From the results, it is concluded that the oblique baffles offers considerable resistance to lateral fluid slosh in the roll plane under lateral acceleration excitation. Furthermore, a higher inclination of the oblique baffles (TO3) tends to enhance the resistance in the roll plane. The conventional lateral baffles, however, exhibit better anti-slosh behavior in the pitch plane than the oblique baffles under simultaneous lateral and longitudinal excitations, although an opposite trend was observed in the roll plane. Further results show that the partial baffles generally ineffective in the roll plane under pure lateral acceleration excitation. The partial baffles with lower partition (TP1) effectively suppress the fluid slosh in the pitch plane for the lower (40%) fill levels, while partial baffles with upper partition (TP2) suppress the slosh under intermediate (60 %) and higher (80 %) fill levels under pure longitudinal and simultaneous lateral and longitudinal excitations. The alternate arrangement of partial baffles ('TP3') tends to considerably suppress the pitch moment, irrespective of the fill levels. The results suggest that further studies in identifying an optimal baffle design would be highly desirable.

## **CHAPTER 5**

### **CONCLUSIONS AND RECOMMENDATIONS**

#### **5.1 MAJOR CONTRIBUTIONS OF THE STUDY**

The fluid slosh within partly-filled tanks is known to be highly non-linear, particularly under severe braking or steering- induced maneuvers. The transient slosh forces and moments caused by a directional maneuver largely depends on the tank and baffles geometry, fill volume and nature of the external excitation. It has been known that conventional lateral baffles provide effective resistance to longitudinal fluid induced by brakes and acceleration maneuvers, while they offer negligible resistance to lateral load transfer, which contributes to the primary overturning moment of partly-filled vehicle. The analyses of antislosh effectiveness of baffles, however, have been limited to a few recent studies, which focus on conventional lateral baffles.

This study proposed alternate concepts in baffles that could affect the fluid slosh in both the roll and pitch planes, which constitutes the major contribution. The study further investigated the nonlinear fluid slosh characteristics of proposed concepts using computation fluid dynamic (CFD) approach. Through systematic analyses of transient as well as steady-state slosh forces and moments under excitations in the longitudinal, lateral axis, the relative antislosh properties of the proposed concepts are presented and discussed in view of varying fill and excitation levels.

## 5.2 MAJOR CONCLUSIONS

The major conclusions of this dissertation research are summarized below:

- Fluid slosh is highly dependent on the tank and baffle configuration, fill volume and nature of the external excitation. Lower fill volume tends to yield greater magnitudes of slosh forces and moments compared to those developed under higher fill volumes.
- The slosh forces and moments exhibit oscillations of considerable magnitudes which decay gradually, while the rate of decay for the cleanbore tank is substantially lower than for the baffled tanks, suggesting greater damping effect of the baffles.
- The anti-slosh effect of conventional lateral baffles is minimal in terms of the lateral slosh force and roll moment caused by a centrifugal acceleration excitation. These baffles, however, can effectively alter the fluid slosh in the longitudinal direction. Under a longitudinal ramp-step acceleration excitation, the pitch moment due to fluid slosh within a cleanbore tank exhibits continuous oscillations, while pitch moment of slosh in a baffled tank yields steady-state value in an asymptotic manner.
- The oscillations in the lateral slosh force and roll moment diminishes rapidly in case of a cleanbore tank, while the roll plane responses for the baffled tank show continued oscillations of considerable magnitudes under simultaneous lateral and longitudinal excitations.

- The fundamental slosh natural frequency depends on the fill volume. This frequency, increased with fill volume in both lateral and longitudinal directions. The addition of lateral baffles causes a significant increase in the longitudinal mode natural frequency, while the lateral mode is not affected.
- The variations in the baffles curvature revealed negligible effect on slosh forces and moments in the roll plane when the tank was subjected to lateral acceleration excitation, but the curvature effect on the pitch plane responses was significant under simultaneous lateral and longitudinal acceleration excitations. Conventional lateral baffles resulted in considerably lower peak lateral slosh force when the tank is subject to a simultaneous lateral and longitudinal ramp-step acceleration excitation. The effect of curvature depth was also found to be negligible.
- The baffle orifice area ranging from 8% to 20% of the tank cross section area covered negligible variations in the peak longitudinal slosh force, but small orifices baffles resulted in lower pitch moment.
- The baffle orifice shape and location are the key factors in controlling the antislosh effectiveness of the baffles. The single half-circle orifice baffle and the half-opened partial baffle were found to be highly effective in reducing the transient pitch moment particularly under intermediate fill volumes. The alternate pattern of partial baffles resulted in significantly lower pitch moment, irrespective of the fill level.

- Oblique arrangement of could provide significant resistance to lateral fluid slosh under lateral acceleration excitations, while the conventional lateral baffles provide most effective antislosh in the pitch plane.

### **5.3 RECOMMENDATIONS FOR FUTURE WORKS**

The present study is considered as preliminary attempt to evaluate the effects different design concepts in baffles on fluid slosh in partly-filled tanks subject to longitudinal, lateral, and combined longitudinal and lateral acceleration excitations. The study, however, is considered to constitute an important step towards building knowledge on the role of various baffle design factors on the resulting slosh forces and to identify the transient fluid slosh characteristics of different baffles considerably more efforts are needed to assess the effectiveness of different concepts in baffle designs and baffles geometry. It was also evident that results clearly suggested that fluid slosh is strongly influenced by the baffles geometry. It is thus recommended to conduct further systematic studies in an attempt to identify optimal baffles designs. Some of the recommended tasks are listed below:

- This study has been limited to the dynamics of the liquid slosh in a moving container, subject to lateral, longitudinal and simultaneous lateral and longitudinal accelerations. These results may be applied to study the vehicle directional characteristics; further efforts in integrating the fluid slosh model to the vehicle model are highly desirable to investigate the baffles effectiveness in the coupled tank-vehicle system.

- The analysis should be extended to include alternate tank cross-sections that are frequently used in bulk liquid cargo transportation. This would permit characterization of the role of the tank geometry and identification of more desirable tank cross-sections and baffles.
- This study has assumed uniform field of acceleration for the liquid. More accurate results could be obtained if non-uniform fields of acceleration arising from turning or braking are considered.
- The experimental slosh investigations for all the baffled tanks configurations are important to validate the model and results.
- The study has shown promising results for the oblique baffles and partial baffles in an alternate arrangement. The combination of the two features maybe highly beneficial for suppressing sloshes in both the pitch and roll planes. Further analyses of oblique partial baffles should thus be conducted.
- Oblique baffles tend to reduce the magnitude of pitch moment by trapping certain amounts of fluid between the consecutive baffles. This is expected to enhance the braking performance of the partly-filled tank vehicles. The designs that limit the roll moment should be explored to enhance the roll stability of partly-filled vehicles.

## REFERENCES

1. Modaressi, K. (2004) "Analysis of transient liquid slosh inside a partly filled tank subjected to lateral and longitudinal acceleration fields " M.A.S.C thesis, Department of Mechanical and Industrial Engineering, Concordia University, Montreal, Canada.
2. Yan, G. (2008), "Liquid slosh and its influence on braking and roll responses of partly filled tank vehicles" Ph.D thesis, Department of Mechanical and Industrial Engineering, Concordia University, Montreal, Canada.
3. Kang, X. D. (2001) "Optimal tank design and directional dynamic analysis of liquid cargo vehicles under steering and braking" Ph.D. thesis, Department of Mechanical and Industrial Engineering, Concordia University.
4. Berlamont, J. and Vanderstappen, N. (1979) "The effect of baffles in a water tower tank" Proc 5<sup>th</sup> Int Conf Wind Eng, Ford Collins, CO.
5. Wang, Z., Rakheja, S. and Sun, C. (1995) "Influence of partition location on the braking performance of a partially filled tank truck" Society of Automotive Engineers, pp. 75-84.
6. Ranganathan, R. and Yang, Y. (1996) "Impact of liquid load shift on the braking characteristics of partially filled tank vehicles" Vehicle system dynamics, vol. 26, pp. 223-240.

7. Ranganathan, R. (1993) "Rollover threshold of partially filled tank vehicles with arbitrary tank geometry" Proc Instn Mech Engrs, Vol 207, Part D, Journal of Automotive Engineering.
8. Salem, M. I. (2000) "Rollover Stability of Partially Filled Heavy-Duty Elliptical Tankers Using Trammel Pendulums to Stimulate Fluid Sloshing" PhD Dissertation, West Virginia University.
9. Sheu, T.W.H. and Lee, S.M. (1998) "Large-amplitude sloshing in an oil tanker with baffle-plate/drilled holes", IJCFD, vol. 10, pp. 45-60.
10. Lloyd, N., Vaiciurgis, E., and Langrish, T.A.G. (2002) " The effect of baffle design on longitudinal liquid movement in road tankers: an experimental investigation " Process Safety and Environmental Protection, Transactions of the Institution of Chemical Engineers, Part B, vol. 80, n 4, July, pp. 181-185.
11. Popov, G., Sankar, S. and Sankar, T.S. (1993) "Dynamics of liquid sloshing in baffled and compartmented road containers" Journal of Fluids and Structures, no.7, pp.803-821.
12. Popov, G. (1991) "Dynamics of liquid sloshing in road containers" Ph.D. thesis, Department of Mechanical and Industrial Engineering, Concordia University.
13. Abramson, H.N., Chu, W.H. and Kana, D.D. (1966) "Some studies of nonlinear lateral sloshing in rigid containers" Journal of Applied Mechanics, Transactions of the ASME, vol.33, no.4, pp.777-784.

14. Budiansky, B. (1960) "Sloshing of liquids in circular canals and spherical tanks"  
Journal of the Aerospace sciences, vol. 27, no. 3 pp. 161-173.
15. Strandberg, L. (1978) "Lateral Stability of Road Container" VTI (The Swedish  
National Road and Traffic Research Institute) Report No. 138A, Sweden.
16. Abramson, R. (1966) "The dynamic behavior of liquids in moving containers",  
1966, NASA, NASA SP-106.
17. Ranganathan, R. (1997) "Development of a roll dynamics model of a liquid tank  
vehicle" Transactions of the CSME, vol. 21, no.4, pp.357-369.
18. Hutton, R.E. (1963) "An investigation of nonlinear, nonplanar oscillations of  
liquid in a cylindrical container" NASA Technical Note D-1870.
19. Berlot, R.R. (1959) "Production of rotation in a confined liquid through  
translational motions of the boundaries" Journal of Applied Mechanics, vol.26,  
TRANS.ASME, vol.81, Series E. pp.513-516.
20. Ranganathan, R. (1990) "Stability analysis and directional response  
characteristics of heavy vehicles carrying liquid cargo" Ph.D. thesis, Concordia  
University, Montreal, Canada.
21. Sankar, S., Rakheja, S. and Ranganathan, R. (1989) "Directional response of  
partially filled tank vehicles" SAE paper, no.892481.
22. Bauer, F. (1981) "Dynamics behaviour of an elastic separating wall in vehicle  
containers" International journal of vehicle design, vol. 2, no. 1.

23. Rakheja, S., Sankar, S. and Ranganathan, R. (1988) "Roll plane analysis of articulated tank vehicles during steady turning" *Vehicle system dynamics*, 17, pp.81-104.
24. Rakheja, S., Sanker, S. and Ranganathan, R. (1989) "Influence of tank design factors on the rollover threshold of partially filled tank vehicles" *SAE Technical Paper Series, Truck and Bus Meeting and Exposition*.
25. Kang, X., Rakheja, S. and Stiharu, I. (2002) "Cargo load shift and its influence on tank vehicle dynamics under braking and turning" *Int. J. of Vehicle Design*, Vol. 9, No. 3.
26. Bauer, F. (1964) "Fluid oscillations in the containers of a space vehicle and their influence upon stability" *NASA, NASA TR R-187*.
27. Uras, R.A. (1995) "Sloshing analysis of viscous liquid storage tanks" *Fluid-sloshing and Fluid-structure Interaction, ASME Pressure and Piping Conf., PVP-vol.314*, pp.63-72.
28. Kang, X., Rakheja, S. and Stiharu, I. (2000) "Effects of tank shape on the roll dynamic response of a partly filled tank vehicle" *Vehicle system dynamics*, Vol. 35, No. 2, pp. 75-102.
29. Popov, G., Sankar, S. and Sankar, T.S. (1996) "Shape optimization of elliptical road containers due to liquid load in steady-state turning" *Vehicle system dynamics*, vol. 25, pp. 203-221.

30. Jitu K., Chiba T., Media T. (1994) " An experimental study of the effect of liquid viscosity on dynamic response of the fluid-filled co-axial cylinder" Sloshing, Fluid-Structure Interaction and Struct response Due to Shock and Impact Loads, ASME Pressure Vessels and Piping Conf., PVP- vol.272, pp.101-110.
31. Su, T.C., Lou, Y.K., Flipse, J.E. and Bridges, T.J. (1982) "A numerical analysis of large amplitude liquid sloshing in baffled containers" Ocean Engineering Program, Texas A&M University, College Station, Texas, USA, Report no. MARD-940-82046.
32. Harlow, F.H., Welch, J.E. (1965) "Numerical calculation of time-dependent viscous incompressible flow of fluid with free-surface" Physics of Fluids, vol.8, no.12, pp.2182-2189.
33. Mikelis, N.E., Miller, J.K. and Taylor, K.V. (1984) " Sloshing in partially filled liquid tanks and its effect on ship motions: numerical simulations and experimental verification" A conference proceeding of The Royal Institution of Naval Architechs, April 11, pp.267-282.
34. Hirt, C.W., Nichols, B.D., and Pomeroy, N.C. (1975) "SOLA – A numerical solution algorithm for transient fluid flows" Los Alamos Scientific Laboratory, Report LA-5852.
35. Navickas, J., Peck, J.C., Bass III, R.L., Bowles, E.B., Yoshimura, N. and Endo, S. (1981) " Sloshing of fluids at high fill levels in closed tanks" ASME Winter Meeting, Washington D.C., pp.191-198.

36. Armenio, V., La Rocca, M. (1995) "Numerical and experimental analysis of liquid sloshing in rectangular containers" Computational Mechanics Publ, pp.11-21.
37. Rumold, W. (2001) " Modeling and simulation of vehicles carrying liquid cargo" Multibody System Dynamics, vol.5, pp.351-374.
38. Sames, P.C., Marcouly, D. and Schellin, T.E. (2002) "Sloshing in rectangular and cylindrical tanks" Journal of Ship Research, vol.46, no.3, Sept., pp.186-200.
39. Okamoto, T. and Kawahara, M. (1990) "Two-dimensional sloshing analysis by Lagrangian finite element method" Int. J. Numerical Methods Fluids, no.11, pp.453-477.
40. Webb, D.C. and Kormi, K. (1999) "The use of the finite element method in the simulation of liquid sloshing" Proceedings of the Ninth International Offshore and Polar Engineering Conference, Brest, France, May 30-June 4, vol.3, pp.615-620.
41. Kondo, N. (2000) "Three-dimensional finite element analysis for incompressible viscous fluid with free surface" Theoretical and Applied Mechanics, vol.49: Proceedings of the 41<sup>st</sup> Japan Congress for Applied Mechanics, pp.127-35.
42. Hadzic, I., Mallon, F. and Peric, M. (2001) "Numerical simulation of sloshing, Proc. SRI-TUHH Mini Workshop on Numerical Simulation of Two-phase Flows" Ship Research Institute, Tokyo, Japan.

43. Hirt, C.W. and Nichols, B.D. (1981) "Volume of fluid (VOF) method for the dynamics of free boundaries" *Journal of Computational Physics*, vol.39, no.1, pp.201-225.
44. Wang, J.P., Borthwick, A.G.L. and Taylor, R.E. (2004) "Finite-volume-type VOF method on dynamically adaptive quadtree grids" *International Journal for Numerical Methods in Fluids*, vol.45, pp. 485-508.
45. Abramson, R (1978) "liquid sloshing dynamics theory and applications".
46. Kobayashi, N., Mieda, T., Shibata, H. and Shinozaki, Y. (1989) "A study of the liquid slosh response in horizontal cylindrical tanks" *Transactions of the ASME, Journal of Pressure Vessel Technology*, vol.111, February, pp.32-38.
47. Pal, N.C., Bhattacharyya, S.K. and Sinha, P.K. (2001) "Experimental investigation of slosh dynamics of liquid-filled containers" *Experimental Mechanics*, vol.41, no.1, pp.63-69
48. Shia, Y. (1969) "Fluid mechanics; a concise introduction to the theory" McGraw-Hill.
49. Fluent User's Guide "Section 22.3.1"
50. Hirt, C.W. and Nichols, B.D. (1981) "Volume of fluid (VOF) method for the dynamics of free boundaries" *Journal of computational physics*, 39, 201-225.
51. Ranganathan, R., Rakheja, S. and Sankar, S. (1990) "Influence of liquid load shift on the dynamic response of articulated tank vehicles" *Vehicle System Dynamics*, Vol.19, No.4, pp.177-200.

52. Gambit documentation "Section 18.3"

53. Heglund, R.E. (1986) "Truck Safety- An agenda for the future" SAE publication

No. P-181, pp. 154-159